Austrian Journal of Earth Sciences | Volume 103/2 | 50 - 80 | Vienna | 2010

Fluvial deposits of the St. Marein-Freischling Formation – insights into initial depositional processes on the distal external margin of the Alpine-Carpathian Foredeep in Lower Austria

Slavomír NEHYBA[1)*)] & Reinhard ROETZEL[2)]

KEYWORDS

St. Marein-Freischling Formation
Oligocene – Lower Miocene
external margin
fluvial deposits
Molasse zone
braided river
Austria

[1)] Institute of Geological Sciences, Faculty of Science, Masaryk University, Kotlářská 2, CZ-611 37 Brno, Czech Republic;

[2)] Geological Survey, Neulinggasse 38, A-1030 Wien, Austria;

[*)] Corresponding author, slavek@sci.muni.cz

Abstract

In the SE Bohemian Massif of Lower Austria sandy and gravelly fluvial strata of the St. Marein-Freischling Formation (Oligocene – Lower Miocene) were deposited in a braided channel system. A network of relatively shallow streams with seasonal fluctuations in the discharge is supposed. Eleven lithofacies and four facies associations/architectural elements (gravelly channel dunes and bars, channels, sandy channel dunes and abandoned channels) were recognised. Provenance studies (pebble petrography, heavy minerals), evaluation of pebble size, shape and roundness, and paleocurrent data point at two separated parts of the fluvial system.

For the main fluvial system a general transport from west to east can be supposed, which finally turned to the south in the surroundings of Horn. Tributaries both from north and south ended in the west-east reach of the main trunk river. Weathered crystalline rocks of the South Bohemian Batholith and the Moldanubian zone (Eisgarn granite, Rastenberg granodiorite, Wolfshof syenitic gneiss, Gföhl gneiss, granulites, marbles, eclogites, amphibolites) are reconstructed as source rocks. However, local sources strongly influenced the provenance spectra.

In a second, probably separate fluvial system in the southeast, a general transport from northeast to southwest is evident, where metamorphic rocks of the Moravian zone, magmatic rocks of the Thaya Batholith, and probably also reworked Mesozoic sediments are the main sources.

For the position and orientation of the paleovalley the tectonic influence of the north-ward thrusting Eastern Alps is discussed, causing a back-bulge depression along the external margin of the foreland basin. Additionally, in the lower reach of the fluvial system (Horn Basin), the position of the paleovalley at the tectonic contact between the Moldanubian and Moravian zones and the reactivation of the fault-system are evident.

Die sandig-kiesigen Ablagerungen der St. Marein-Freischling-Formation (Oligozän – Untermiozän) in der südöstlichen Böhmischen Masse in Niederösterreich wurden in einem fluviatilen braided-river System abgelagert.

Ein relativ seichtes Flussnetz mit verzweigten Rinnen (braided channels) und saisonal bedingten, schwankenden Abflussraten wird angenommen. 11 Lithofazies-Typen und vier Fazies-Assoziationen (gravelly channel dunes and bars, channels, sandy channel dunes, abandoned channels) konnten unterschieden werden. Aufgrund der Untersuchungen der Sedimentherkunft mit Hilfe von Geröllpetrographie und Schwermineralen, der Auswertung von Größe, Form und Rundungsgrad der Gerölle, sowie der Paläoströmungsdaten lassen sich grundsätzlich zwei getrennte fluviatile Systeme unterscheiden.

Im Hauptbereich des fluviatilen Systems kann ein Transport von West nach Ost festgestellt werden, der sich im Bereich von Horn gegen Süden wendet. Seitliche Nebenflüsse mündeten von Norden und Süden in den West-Ost orientierten Bereich des Hauptflusses. Das Sedimentmaterial stammt von verwitterten kristallinen Gesteinen des Südböhmischen Batholiths und des Moldanubikums. Vorwiegend wurde das Material vom Eisgarner Granit, Rastenberger Granodiorit, Wolfshofer Syenitgneis oder Gföhler Gneis und von Granuliten, Marmoren, Eklogiten und Amphiboliten geliefert, aber auch andere lokale Einflüsse konnten festgestellt werden.

Im zweiten, wahrscheinlich eigenständigen fluviatilen System im Südosten mit einem vorherrschenden Transport von Nordost nach Südwest stammt das Sedimentmaterial vorwiegend von moravischen Metamorphiten, granitischen Gesteinen des Thaya-Batholiths und eventuell auch umgelagerten mesozoischen Ablagerungen.

Lage und Orientierung des ehemaligen Flusstales haben möglicherweise einen tektonischen Hintergrund in Zusammenhang mit den nordwärts aufschiebenden Ostalpen, wodurch eine back-bulge Depression entlang des externen Randes des Vorlandbeckens induziert wurde. Im unteren Bereich des Flusstales, im Horner Becken, sind außerdem die Lage am tektonischen Kontakt von Moldanubikum und Moravikum und die damit verbundene Reaktivierung des dortigen Bruchsystems offensichtlich.

1. Introduction

Analysis of fluvial systems and its paleodrainage provide crucial data for the reconstruction of ancient landscapes and

paleogeography (e.g. Gupta, 1997). Paleovalley systems which cut into the bedrock are fundamental components of the stratigraphic record, often connected with important unconformity surfaces. The interaction between tectonic and surface processes is responsible for the driving of the fluvial network. The angle of the slope plays the most significant role for the formation of drainage and channel direction. The fluvial transport is quite important in the determination of the asymmetry of the foreland basin geometry (Johnson and Beaumont, 1995) where the concept of lithospheric flexure as the principal basin formation mechanism is widely accepted (Beaumont, 1981; Jordan, 1981; Allen et al., 1986; Johnson and Beaumont, 1995; etc.). Peripheral foreland basin systems provide several discrete depozones (DeCelles and Giles, 1996) with varied orientation of the slope. Continuous loading of the thrust wedge onto the flexed passive margin led to the continuous shift of the depozones and slope orientation. For that reason relations of the formation of the foreland incised paleodrainage network to the evolution of the flexural basin represent important information.

The deposits of St. Marein-Freischling Formation (SMFF), which cover the crystalline basement of the Bohemian Massif in the area of northwestern Lower Austria (Fig. 1), provides a typical example of such a situation. The position of the SMFF below the basal/forebulge unconformity (Crampton and Allen, 1995) of the Austrian Molasse Zone allows us to study the drainage system and formation of paleovalleys in the foreland prior to a flexurally induced transgression.

The main objectives of the study are: 1) description of the deposits of the SMFF with respect to the depositional environment, 2) reconstruction of the paleodrainage pattern with respect to the provenance, and 3) evaluation of the controls on incision of the paleovalley.

2. Geological setting

In northwestern Lower Austria coarse-grained clastic sediments can be found in a belt-like distribution above crystalline rocks of the southeastern Bohemian Massif (Fig. 1). These sediments of the St. Marein-Freischling Formation (SMFF) are widespread in the tectonically induced L-shaped Horn Basin and extend to the west up to the Gmünd area. The formation is named after two villages in the main distribution area in the Horn Basin (Fig. 1).

The name of the formation was first introduced by Steininger (1983: p.24) and afterwards used in the geological map sheet 20 Gföhl (Fuchs et al., 1984). These sediments were defined by Steininger and Roetzel (1991) and later on specified in Roetzel et al. (1999).

For the SMFF no type section was defined up to now. Infor-

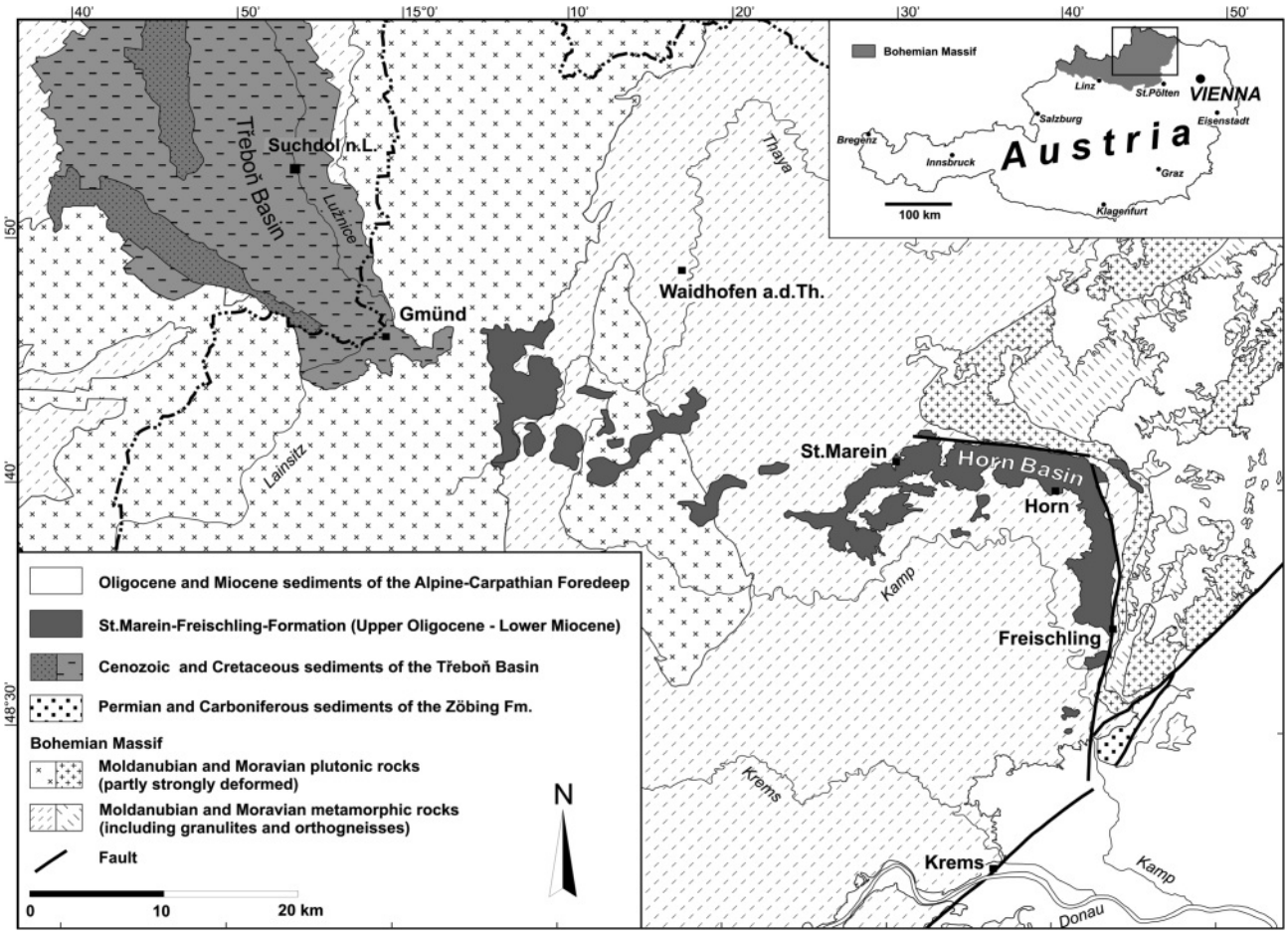

Figure 1: Simplified geological map of the Bohemian Massif in Lower Austria and adjacent Czech Republic and the extension of the St. Marein-Freischling Formation (SMFF) (using the geological map of Lower Austria 1:200.000; Schnabel et al., 2002).

mally, as reference sections, a sandpit 1 km SW of St. Marein (outcrop 12), a sandpit 1.3 km SE of Breiteneich (outcrop 21; Roetzel and Steininger, 1991), the abandoned clay-pit Maiersch (Frings, outcrop 29) 1.5 km ENE of Maiersch (Steininger, 1976, 1977: p.75 ff., 1983; Steininger et al., 1991a), and the sandpit Obernholz-Gemeindesandgrube (outcrop 32; Steininger, 1977: p. 72 ff., 1983; Steininger et al., 1991b) can be regarded (cf. Fig. 2, Tab. 1). The upper boundary of the SMFF is exposed in the sandpit Obernholz; formerly it also was exposed in the today abandoned clay-pit Maiersch.

These sediments are already shown in the geological map of Čžjžek (1849), who described them as Tertiary gravel and sand (Čžjžek, 1853). Suess (1866) mentioned unfossiliferous sand and clay in the surroundings of Horn, and Schaffer (1914) recognised the fluvial character of these poorly sorted clayey sand and gravel in the Horn Basin deposited by a pre-Miocene river system ("Horner Strom"). Ellenberger (1948) and his colleagues studied this fluvial sedimentary cover with silicified wood and reworked Jurassic belemnites in detail in the prisoner-of-war camp in Edelbach. Waldmann (1951) first recognised the sediments as a fluvial drainage of the South Bohemian Třeboň Basin across the recent main European watershed and dated the deposits to the Oligocene. In earlier papers by Steininger (1968a, b, 1969, 1976, 1977, 1979), who mapped the sediments in the Horn Basin, they were named "Fossilleere Serie", "Fossilarme Serie" or "Kontinentale Serie".

Sediments of the SMFF are badly sorted arkosic and pelitic, coarse to fine sand and gravel with intercalations of kaolinitic silt and clay, showing typical sedimentary structures of a fluvial environment. A detailed granulometric and mineralogical description of the SMFF is given by Wimmer-Frey (1999).

The sediments of the SMFF are mainly fluvial deposits from a river system draining the Třeboň Basin in South Bohemia and the southeastern Bohemian Massif in the Oligocene to Early Miocene (Kiscellian to Egerian) from northwest to southeast. A confluence to the Oligocene sea and the interfingering with sediments of the Linz-Melk Formation can be supposed in the Krems area (Fig. 1; Roetzel et al., 1999; cf. Fig. 19).

In the Horn Basin about 100 to 150 m of SMFF sediments are reported by hydrological drillings, forming a very important reservoir for groundwater (Herndler, 1979). The tectonical induced asymmetric structure of the Horn Basin is proven by these drillings and also by geophysical data (Scheidegger et al., 1980;

No.	name of outcrop	ÖK-sheet	BMN-coordinates M34	
			x-coordinates	y-coordinates
1	Kirchberg – Rote Kapelle	19 Zwettl	659098	399962
2	Kirchberg-7 drilling	19 Zwettl	661484	399523
3	Süßenbach	19 Zwettl	661289	398220
4	Mayerhöfen	19 Zwettl	664018	395761
5	Großglobnitz	19 Zwettl	663847	395118
6	Sandholz	19 Zwettl	674062	390434
7	Sandholz-SE	19 Zwettl	674701	389937
8	Thaures	20 Gföhl	680221	390381
9	Thaures-E	20 Gföhl	680472	390332
10	Mestreichs	20 Gföhl	683334	390083
11	Altpölla	20 Gföhl	687046	387425
12	St. Marein	20 Gföhl	687736	394121
13	Frankenreith	20 Gföhl	689282	393399
14	Fürwald	20 Gföhl	690875	394356
15	St.Bernhard	20 Gföhl	694465	394267
16	Altenburg	21 Horn	695100	391307
17	Nödersdorf	21 Horn	697101	400649
18	Frauenhofen	21 Horn	698073	394595
19	Himmelreich	21 Horn	700797	394354
20	Breiteneich-Wienerberger	21 Horn	702703	393980
21	Breiteneich	21 Horn	703685	392131
22	Mold-Sandhölzl	21 Horn	702885	390741
23	Rodingersdorf-A	21 Horn	705511	393670
24	Rodingersdorf-B	21 Horn	705650	393370
25	Klein-Meiseldorf-6 drilling	21 Horn	706055	392920
26	Klein-Meiseldorf	21 Horn	706656	392406
27	Zaingrub	21 Horn	703399	387885
28	Nonndorf excavation	21 Horn	704752	385006
29	Maiersch	21 Horn	704030	382770
30	Freischling	21 Horn	704073	382036
31	Ravelsbach 1,2,3	21 Horn	710278	379057
32	Obernholz	21 Horn	706114	375233

Table 1: List of studied outcrops of the St. Marein-Freischling Formation (cf. Fig. 2).

Ahl, 2000, 2003). West of the Horn Basin the thickness of these deposits decreases to usually 20 m to 65 m.

Sediments of the SMFF mostly are overlying unconformably above the crystalline basement rocks of the Bohemian Massif. In the Gmünd area it can be supposed that the Upper Cretaceous Klikov Formation is lying below the SMFF. In the southern Horn Basin, the SMFF is gradationally passing over into the Lower Miocene (Eggenburgian) Mold Formation but in many parts it is overlain unconformably by Pleistocene sediments.

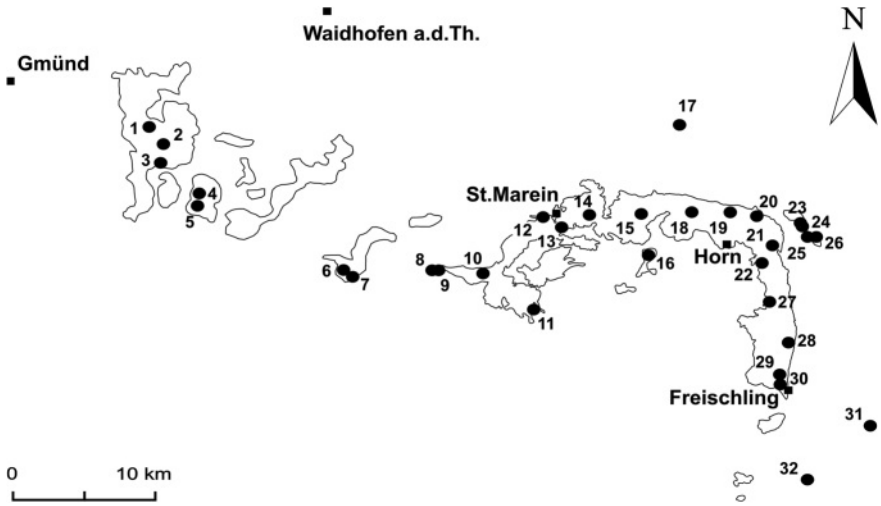

Figure 2: Position of the studied outcrops of the SMFF (cf. Table 1).

It has to be assumed that the Beds of Freistadt-Kefermarkt in Upper Austria are facies- and time-equivalent deposits of the SMFF (cf. Chábera and Huber, 2000).

In the sandy and gravelly sediments of the SMFF silicified wood is common (Hofmann, 1933; Ellenberger, 1948; Gros, 1981, 1983, 1984, 1988; Cichocki, 1988), wheras in pelitic layers remnants of leave impressions (Knobloch, 1977, 1981), pollen, and spores (Hochuli, 1983) occur. Fossil plant species from Horn, represented by leaves of *Sequoia abietina*, T*axodium dubium*, *Populus hornensis*, *Zelkova*, and *Acer*, are dated due to the archaic Populus-species by Knobloch (1981) to the Oligocene to lowermost Miocene (Egerian).

The pollen-flora of clayey sediments of the SMFF was dated to the Pollenzones Pg.Z. 19, Pg.Z. 20a, Ng.Z.I, and Ng.Z.II (Hochuli, 1983). Due to these pollen data a correlation with the Oligocene and lowermost Miocene (Kiscellian – Egerian, respectively Rupelian – Chattian) is possible.

3. Methods of study

The paper is based on the study of 32 localities. A list of outcrops is shown in Tab. 1 and their location in Fig. 2. Besides sediments from the main distribution area of the SMFF one outcrop in a possible tributary (No. 17) and two outcrops in the southeast with fluvial sediments of unclear lithostratigraphic position (No. 31 and 32) were included into the study. The highly varying quality and accessibility of individual outcrops were one of the reasons for using a combination of wider spectra of sedimentological techniques to fulfil the aims of the study. However, not all these techniques could be applied in all localities.

Lithofacies analysis and paleocurrent studies follow the methods of Tucker (1988), Walker and James (1992), and Nemec (2005). The maximum pebble size was obtained by the measurement of the longest axis (A-axis) of the 10 largest found extraclasts at one lithology (D10-value). Pebble shape and roundness were determined by classifying about 100 quartz clasts in the grain size fraction 8 – 16 mm (sieve separation) at 16 outcrops (4, 6, 8, 9, 10, 11, 12, 13, 14, 18, 21, 23, 24, 30, 31, 32). Shape and roundness were estimated visually using the method of Powers (1982).

Pebble petrography was determined in the grain size fraction > 8 mm classifying between 60 and 339 pebbles in 16 outcrops (4, 6, 8, 9, 10, 11, 12, 13, 14, 18, 21, 23, 24, 30, 31, 32).

Grain size analyses were carried out from 133 samples from all localities except locality 13 and 25 by wet sieving and by using a Sedigraph for grain sizes < 0.063 mm.

The modal composition of sands was studied in 47 samples from 13 localities (6, 9, 11, 12, 16, 18, 21, 23, 24, 29, 30, 31, 32). These studies were done in the grain size fraction 0.063 – 0.5 mm. Several samples from each locality were correlated to the sedimentary logs in the outcrops. Heavy minerals were studied in 118 samples from 27 localities (1-6, 8-12, 14-21, 23, 24, 26, 27, 29-32). A minimum of 100 heavy mineral grains were analysed in each sample. Detailed studies of zircon characteristics were done in 14 selected localities (1-5, 9, 12, 14, 17-19, 21, 24, 31). Outer morphology, colour, presence of older cores, inclusions and zoning were evaluated in the whole zircon spectra under binocular microscope on 1389 grains (e. g. Pupin, 1980). The study of typology (348 grains) and elongation (707 grains) were done only on euhedral or subhedral zircon grains.

The mineral compositions were determined using the Cameca SX 100 electron microprobe at the Joint Laboratory of Electron Microscopy and Microanalyses of the Masaryk University and the Czech Geological Survey Brno. Chemistry of monazite was studied in samples from locality 24 (16 analyses of 7 monazite grains). Chemistry of garnet was analysed for 37 grains from outcrops 10, 11, 17, 31, and 32. Chemistry of rutile is based on data from 56 grains from outcrops 2, 5, 6, 10, 11, 14, 17, 18, 21, 31, and 32. The microprobe study of spinels was obtained for 20 grains from localities 1, 2, 5, 6, 10, 11, 14, 18, 21, and 31. Chemistry of tourmaline was studied in 10 grains from outcrops 5, 6, 14, and 18.

4. Pebble size, shape and roundness

The evaluation of the maximum pebble size did not reveal

any significant trend in the area under investigation. The largest clasts of about 10 cm were recognised mainly in the western localities. Quartz forms the absolute majority of maximum clasts (6.5 - 10 cm) in the investigated localities. Large pebbles and small cobbles (5.5 - 10 cm) of granites (outcrops 9, 10), paragneisses (outcrop 30) and chert (outcrop 32), or pegmatitic quartz and feldspar aggregates (outcrops 11, 12, 13, 21) sometimes also were recognised. Their size usually is in relation with co-occurring quartz pebbles. Mudstone intraclasts appeared in the majority of outcrops. They are often significantly larger than the associated extraclasts, similarly like weathered relics of wood trunks, which were also recognised in some outcrops. Maximum sized pebbles, outsized intraclasts and trunks are absolutely predominant at the base of gravelly beds.

Although both roundness and shape of clasts are related to lithology, they also can be related to the duration, mode and distance of transport (Mills, 1979; Lindsey et al., 2007). The evaluation of the pebble shape and roundness are presented in Fig. 3. Spherical clasts form 33 - 69%, prismoidal 8 - 34% and discoidal 8.3 - 47.7% of the clast spectra. Spherical shape of quartz pebbles clearly dominates in the majority of outcrops. Only in outcrop 32 discoidal and in outcrop 31 prismoidal shapes slightly prevailed. A slightly higher content of prismoidal and discoidal pebbles compared to spherical ones can be recognised in the localities 30, 31, 32, and 12.

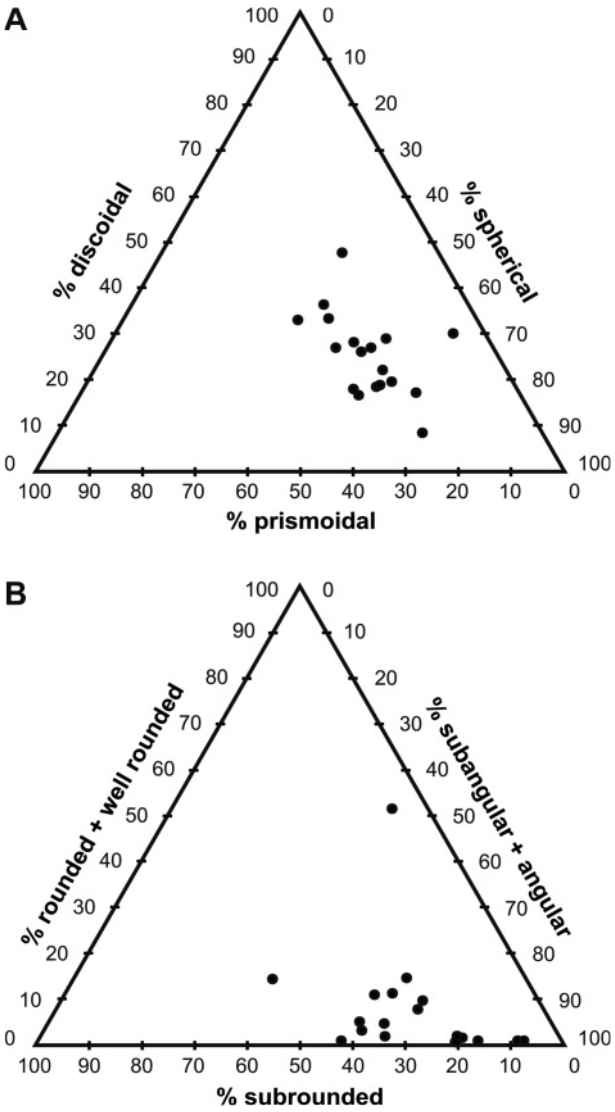

Figure 3: Pebble shape (A) and roundness (B) from the SMFF (method after Powers, 1982).

Quartz pebbles are in the majority of the localities dominantly subangular (forming 24.4 - 82.4%), but also subrounded pebbles are common (forming often more than 20%). Only in the localities 11, 31 and 32 subrounded resp. rounded pebbles are prevailing (forming 41.8 - 51.8%), but subangular pebbles are here also common (forming 24.3 - 35.9%). Angular quartz pebbles form 0.8 - 23.3%. The highest content of angular quartz pebbles was recognised in outcrops 10, 12, 30, and 32, whereas the lowest one was found in outcrops 11, 13, 23, and 31. Rounded quartz pebbles form 0 - 51.8%, but usually up to 14%. Their presence was higher than 10% in outcrops 10, 11, 23, and 32, whereas they were absent in outcrops 14, 18, 30, and 31.

Interpretation: The maximum pebble size distribution seems to support in general a transport from west to east, with some exception for selected outcrops. Significantly coarser basal parts of the bed compared to its major parts reveal a deposition under the highest flow discharge and/or in the deepest part of the channel. The occurrence of outsized extraclasts and wood trunks may indicate a “relative deficiency” of the coarsest grains in the source area.

The distribution of shape and roundness of gravel sized pebbles is complex in the studied area. It may be with a result of multiple sources and minor affection of pebble shape and roundness by fluvial transport. The principal source of pebbles was the weathered crystalline basement, whereas older sedimentary rocks (e.g. Cretaceous sediments) play a minor role or their influence can be followed only in selected outcrops. Remarkable different are the results for the outcrops 31 and 32 where local bedrock significantly influenced the pebble spectra. The existence of a complex fluvial system or fluvial systems can be supposed. Although the roundness of most lithologies (typically quartz) initially increases with downstream transport, it commonly reaches a limiting value (Sneed and Folk, 1958; Lindsey et al., 2007). Roundness in some cases can even decrease downstream (Lindsey et al., 2005).

5. Provenance study

The study of pebble lithology, composition of sands and heavy minerals all belong to the traditional methods of provenance analysis (Dickinson, 1985; Pettijohn et al., 1987; Lihou and Mange-Rajetzky, 1996). The lithology and relief of the source area as well as type and duration of the weathering processes affect the size and lithology of clasts available for transport. The hydraulic character of the drainage (size, gradient and discharge characteristics) determines the rate and distance of transport, degree of recycling, weathering, and ultimate survival of various lithologies. Local outcrops may contribute to the clast population along the fluvial course. Tributaries to the main stream and redeposition of older strata can also contri-

bute to the clast populations and the commingled populations are then transported farther downstream. As a result multi-cycle clast populations are known in many fluvial systems and have long complex histories (Lindsey et al., 2007).

5. 1 Grain size of sediments

Grain size distribution mainly is used for the classification of sediments but it is also a valuable method for calculating the hydrodynamic energy.

The results of 133 grain size analyses are shown in triangle diagrams (cf. Füchtbauer, 1959; Müller, 1961; Fig. 4a-c). Most of the sediments analysed have very small gravel content below 1%. Sediments up to 10% gravel content were plotted in the triangle gravel+sand – silt – clay (Fig. 4a, b). Sediments with gravel content > 10% are shown in the triangle gravel - sand – silt+clay (Fig. 4c).

The sediments of the SMFF predominantly are sands, in minor portions also silty sands and clayey sands. Sands are mainly medium to coarse sands, whereas fine sands are rare. Additionally silt-sands, clay-sands, clayey silt-sands, silty clay-sands, and clayey sand-silt occur (Fig. 4a, b). The coarse sediments mostly can be classified as gravelly sands and gravel-sands; however, some are plotting in the fields of sand-gravel, silty gravel-sand and silty sand-gravel (Fig. 4c). In the coarse fraction fine gravel up to 6.3 mm is dominating, whereas the medium gravel fraction between 6.3 and 20 mm is subordinate. Pelitic intercalations of the SMFF mostly are sandy clay-silts and sandy silt-clays, subsidiary also silt-clays (Fig. 4a, b). Pelitic sediments with gravelly components > 10% are gravelly silt-sands and gravelly sand-silts (Fig. 4c).

According to the classification of Folk and Ward (1957) most of the sediments are extremely poorly sorted (standard deviation σ 2.66 – 6.93) or very poorly sorted (σ 2.58 – 2.01), only few of them are poorly sorted (σ 1.42 – 1.99) or moderately sorted (σ 0.99 – 1.39).

Interpretation: There are three distinct groups of sediments in the SMFF. The main group with sands has low pelitic fractions, pointing to high flow velocity and transport energy. However, the boundary towards the second group with a higher portion of pelitic components but also a substantial amount of gravel and sand is indistinct. This group represents the region with fluctuating transport energy. The third group with a high portion of fine-grained material but in many cases also a considerable coarse fraction is more outstanding and defines areas where low transport energy prevails. However, presumably small amounts of coarse-grained material from connected high current velocity areas were incorporated.

A further significant result from grain size analysis is the exceptional position of most of the sediments from the southeastern part. Especially sediments from outcrop 32 have a lower pelitic content and are better sorted, whereas the analysed samples from outcrop 31 fit better into the general SMFF pattern.

5. 2 Petrography of pebbles

The general results of pebble petrography are presented in

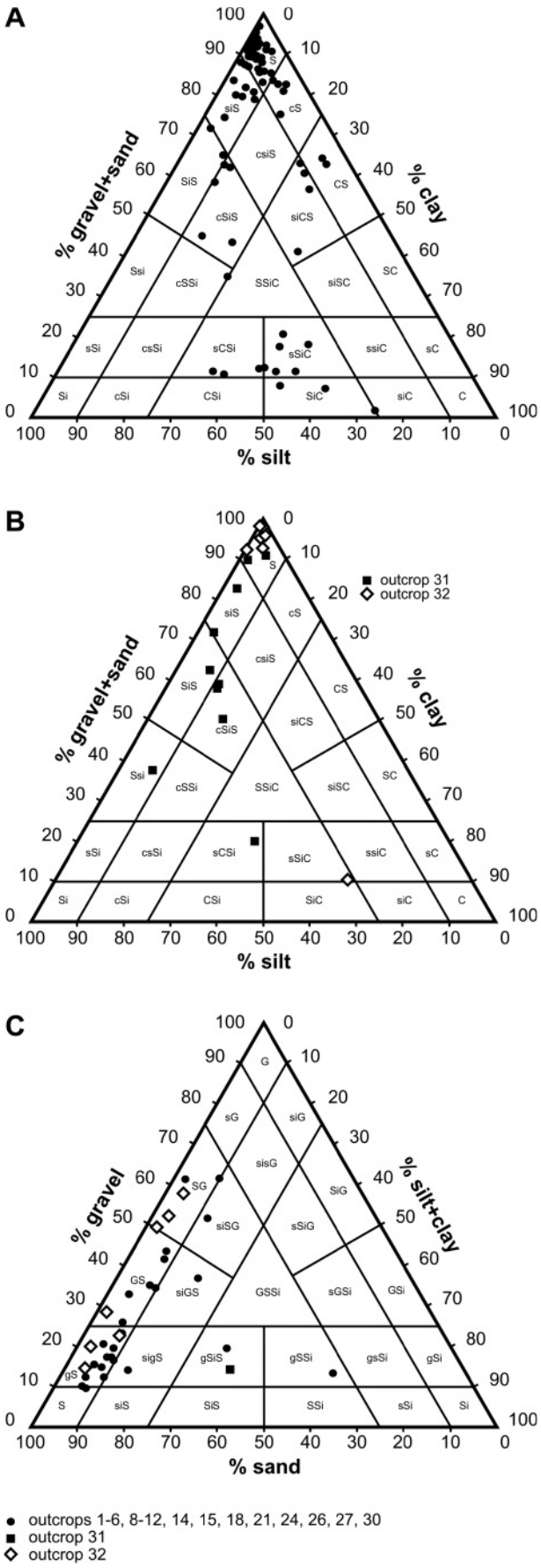

Figure 4: Grain size-based nomenclature of sediments from the SMFF after Füchtbauer (1959) and Müller (1961). (A) outcrops 2-3, 5-7, 9, 11-12, 14-24, and 26-30. (B) outcrops 31 and 32. (C) outcrops 1-6, 8-12, 14, 15, 18, 21, 24, 26, 27, and 30-32.

Fig. 5. The gravel can be classified as polymict to quartzose ones. Quartz pebbles predominate and usually exceed 70%; however, their content strongly varies from 47.6 to 91.7%. Various quartz varieties are present. Whitish, milky quartz is the main type, whereas dark or light grey and pinkish ones occur subordinately. Quartz+feldspar aggregates (rock fragments) were recognised in almost all outcrops forming up to 52.4%. Feldspar is kaolinized. Pebbles of granitic rocks were also found in the majority of outcrops forming up to 12.7%, similarly as gneisses (up to 14.5%). Orthogneisses dominate to the west and paragneisses more often occur to the east of the studied area. Further rock types, such as quartzite, granulite, mica schist, aplite, quartzose sandstone additionally are present (max. 3.4 %). Remarkable are chert pebbles in outcrop 32 (14.1%) and feldspar phenocrysts in outcrops 6 and 8 (2-20%).

Interpretation: The petrography of pebbles reflects the relative high maturity of the SMFF deposits. The provenance was significantly influenced by the local basement composition. The absolute dominance of quartz or quartz+feldspar aggregates (rock fragments) with kaolinized feldspar in all outcrops reflects the provenance from weathered crystalline rocks (granites, orthogneisses) and regolith was the most important source. A minor role of older sedimentary rocks (e.g. chert, which might be Mesozoic in age) can also be supposed. Changes in the basement geology are reflected in the pebble petrography in the studied area from west to east. The provenance from the South Bohemian Batholith (especially from the Rastenberg granodiorite) clearly can be retraced in the outcrops 6, 8, 9, 10, 11, 12, and 14. The provenance from metamorphics of the Moldanubian zone can be verified in the outcrops 8, 9, 10, 11, 12, 13, 14, 18, 21, 23, 24, and 30. Its role generally increases towards the east, which can be documented by a wider spectrum of the gneisses and the occurrence of paragneisses in outcrop 30. Pebbles in outcrop 32 reveal significant differences in the provenance (i.e. older deposits, metamorphic rocks of the Moravian zone, and granitic rocks of the Thaya Batholith).

5. 3 Petrographic composition of sands

The diagram of the modal composition of the studied sands of the SMFF is presented in Fig. 6. The studied samples reveal a highly varied mineralogical maturity. The content of quartz varies between 33.1 - 96.1%, usually above 50%. The content of feldspar grains is between 0.6 - 40.5% (usually above 20%), and the content of lithic fragments varies between 2.7 - 41.1%. The majority (52.9%) of the samples can be classified as arkosic arenites or lithic arenites (27.5%) (e.g. Pettijohn et al., 1987). Only one sample (outcrop 29) can be classified as quartz arenite. Samples from outcrops 29, 31, and 32 on average reveal a higher content of quartz than the rest of the outcrops. Wimmer-Frey (1999) observed the dominance of lithic/composite quartz fragments over single grains, the dominance of alkali feldspar and the absence of carbonates within the SMFF deposits.

Interpretation: These results can be interpreted as evidence for the principal source from weathered crystalline rocks of the South Bohemian Batholith and the Moldanubian zone, and possible local variations in the source rocks for individual outcrops in the area under study (especially in west-east direction).

5. 4 Heavy mineral studies

Heavy minerals are sensitive indicators of the provenance but

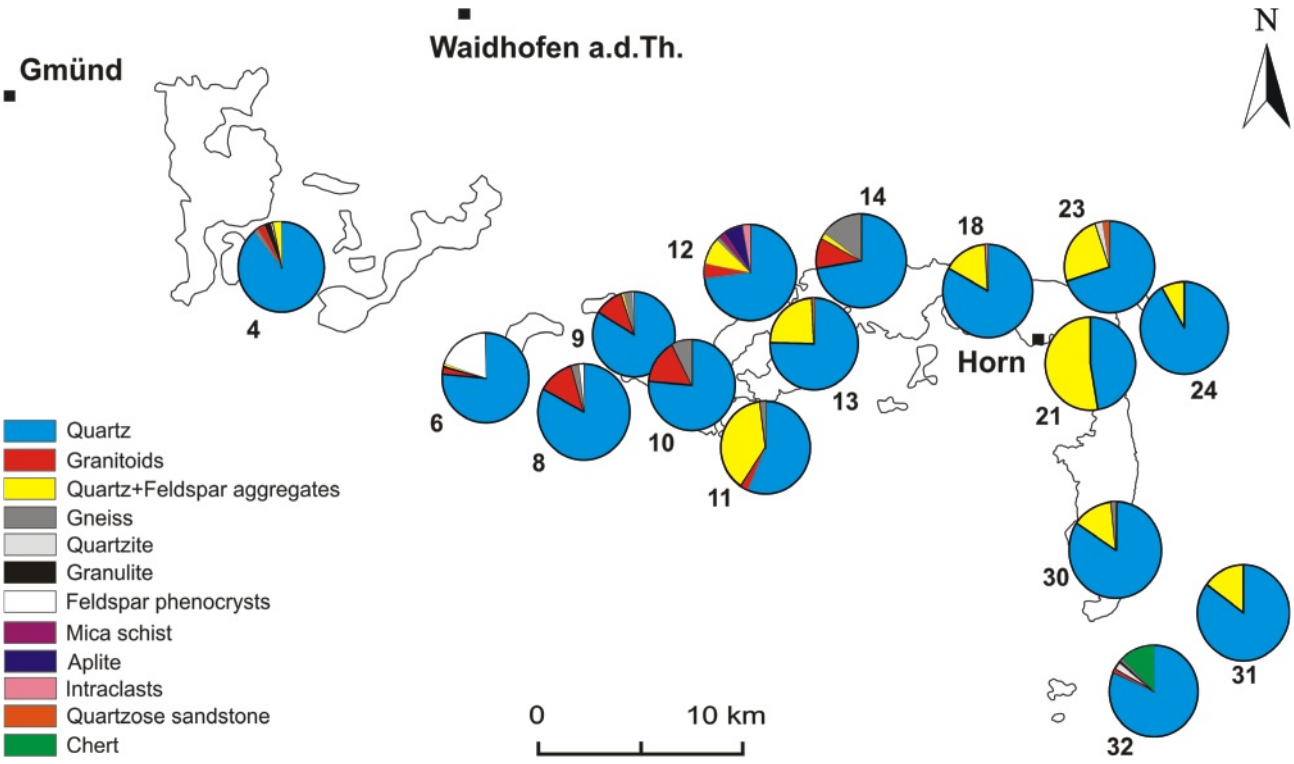

Figure 5: Pebble and cobble petrography (in percentage scale) of the SMFF. For position of the outcrops refer to Fig. 2.

also of the conditions of weathering, transport, deposition, and diagenesis. Probably the most effective method for the evaluation of all factors influencing the heavy mineral spectra is the combination of the study of the heavy mineral assemblages and the ratios of the abundance of minerals with similar hydraulic behaviour (Morton and Hallsworth, 1994) with the chemistry of selected heavy minerals (Morton, 1985, 1991). The heavy mineral ratios apatite/tourmaline (ATi), garnet/zircon (GZi), TiO_2-group/zircon (RZi) and monazite/zircon (MZi) have been used.

5. 4. 1 Heavy mineral assemblages and mineral ratios

The heavy mineral assemblages significantly differ between various localities of the SMFF, but some differences were recognised even within various beds of the same locality. Fluctuations in heavy mineral proportion between samples from a single locality probably reflect the hydraulic conditions during deposition (Morton, 1985).

Localities can be subdivided into six spatially restricted groups (A-F) according to the spectra of translucent heavy minerals, value of mineral ratios and positioning in the area under study (Fig. 7).

Group A is restricted to outcrops 1 and 2 and is located in the westernmost part of the area under study. The highest content of zircon in all groups, as well as tourmaline, sillimanite, kyanite, and rutile are generally typical for this group. The average ATi-ratio is 0, GZi-ratio 12.1, RZi-ratio 30.5, and MZi- ratio 6.1.

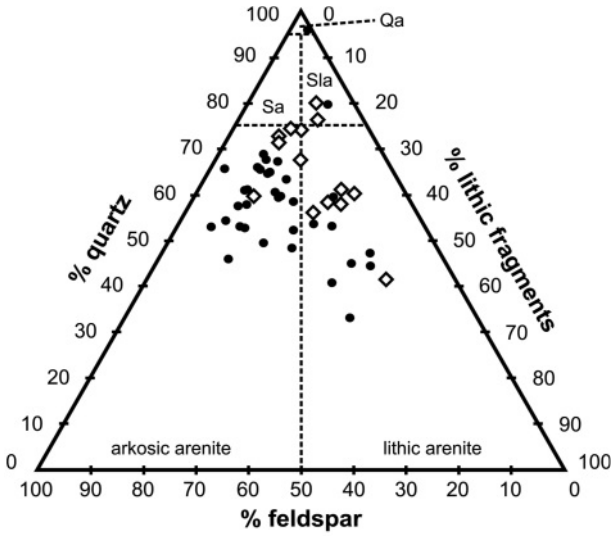

Figure 6: QFL diagram (after Pettijohn et al., 1987) of sands of the SMFF.

Group B is defined by outcrops 3, 4, 5, 6, 8, 9, 10. An association of heavy minerals with high contents of sillimanite, tourmaline, kyanite, rutile, and zircon is typical. However, the content of zircon and rutile is significantly lower than in group A, whereas the content of sillimanite and tourmaline is highest for all selected groups. The content of kyanite is also markedly high. However, a higher content of garnet, hornblende and epi-

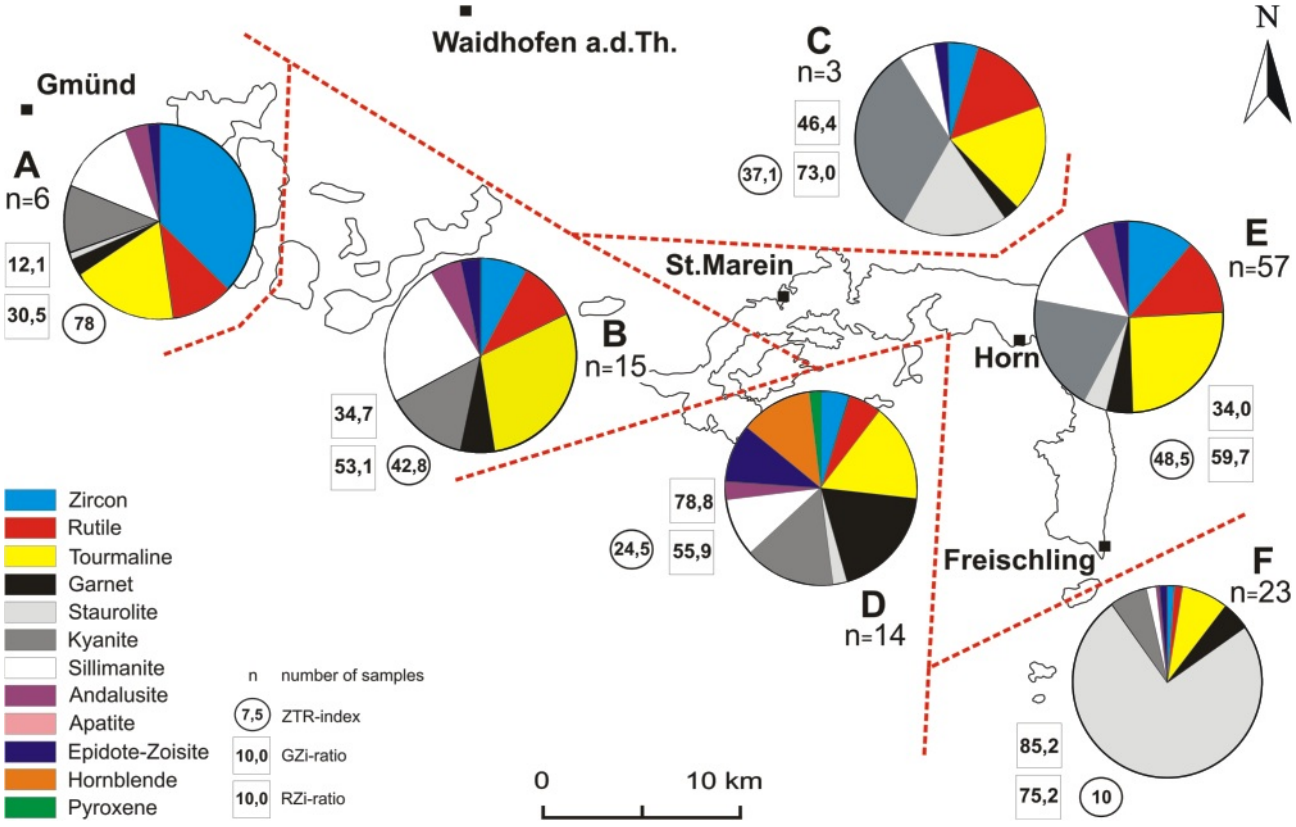

Figure 7: Heavy mineral assemblages A-F (average composition in grain-%) of the SMFF subdivided into areal restricted groups.

dote and a low content of kyanite were also recognised in some samples from outcrop 8. The average ATi-ratio is 0.6, GZi-ratio 34.7, RZi-ratio 53.1, and MZi-ratio 0.

Group C is restricted to outcrop 17, which is the northernmost studied one. The heavy mineral association is typical with an important role of kyanite, tourmaline, staurolite, and rutile, and in some samples also zircon. The content of kyanite was the highest one in all groups. The average ATi-ratio is 0, GZi-ratio 46.4, RZi-ratio 73.0, and MZi-ratio 0.

Group D comproses of localities 11 and 16. A significant amount of garnet, tourmaline, kyanite, sillimanite, hornblende, and in some cases also zoisite and zircon is typical. The contents of hornblende, pyroxene and zoisite are the highest in this group. The average ATi-ratio is 0.1, GZi-ratio 78.8, RZi-ratio 55.9, and MZi-ratio 0.6.

Group E includes the majority of outcrops (i.e. 12-15, 18-21, 23, 24, 26, 27, 29, and 30). Tourmaline, kyanite, zircon, rutile, and sillimanite are dominant in those heavy mineral associations. In some samples also the content of andalusite, staurolite, and epidote is remarkable. The average ATi-ratio is 0.3, GZi-ratio 34.0, RZi-ratio 59.7, and MZi-ratio 0.8.

Group F was selected for outcrops 31 and 32 (in the southernmost part of the area under study). Here the absolute dominance of staurolite is typical, besides tourmaline, garnet, kyanite, and rarely epidote and zircon. The average ATi-ratio is 0.9, GZi-ratio 85.2, RZi-ratio 75.2, and MZi-ratio 3.3.

The ZTR (zircon+tourmaline+rutile) index is widely used as criterion of mineralogical „maturity“ of heavy mineral assemblages (Hubert, 1962; Morton and Hallsworth, 1994). The values of the ZTR-index significantly vary for the studied samples and groups. Samples from outcrops 31 and 32 reveal the lowest ZTR-index (7.5 - 12.4), whereas all other localities have values significantly higher (17.9 - 97), usually scattering around 50. The distribution of the ZTR-index in the studied area can be followed in Fig. 7.

Interpretation: A source from reworked older sediments (probably from Upper Cretaceous deposits of the Klikov Formation; see below) and granitic rocks is supposed for the deposits of group A while for group B a significant input from high-grade metamorphic rocks (granulites, gneisses) and granitic rocks is postulated. For group C an important portion of high- and middle-grade metamorphic rocks (mica schists, gneisses, granulites) in the source area is evident. Group D significantly reveals contribution from basic igneous rocks. Regional occurrences of garnet-pyroxenic amphibolites, granulites and Wolfshof syenitic gneiss in the surroundings of St.Leonhard am Hornerwald probably represent the principal source. The heavy mineral assemblages of Group E point to high-grade metamorphic rocks and granitic rocks in the source area. Some similarity of group B and E can be ascribed to a similar source (Moldanubian zone, South Bohemian Batholith) and a transport direction generally from W to E. An important input of middle-grade metamorphic rocks, especially metapelites, probably from the Moravian zone, can be documented for the group F. An influence of granitic rocks in the provenance is supposed for the majority of the studied samples. The presence of andalusite confirms a source from felsic igneous rocks, maybe from the Eisgarn granite (Slánská, 1967; D'Amico et al., 1982/83; Clarke et al., 2004). The absence or very low content of apatite (together with amphibole, epidote and pyroxene) in the majority of outcrops and the low ATi-ratio can be explained by apatite instability in low ph-groundwaters and modification of its content by weathering (Morton, 1991; Morton and Hallsworth, 1994). The rise of the GZi- and RZi-ratio from west to east and south reflects a continuous increase of a provenance from metamorphic rocks and influence of local sources. It is in good agreement with paleocurrent data (see chapter 6.4). The value of the MZi-ratio generally is very low due to the very low content of monazite, which varies between 0 up to 5.4%. The highest values of MZi-ratio were recognised for group F and A.

Weathered crystalline rocks and polycyclic detritus can explain the high values of the ZTR-index, whereas its lower values in the south can indicate a higher importance of first cycle detritus. The role of the individual minerals (i.e. zircon, tourmaline and rutile) on the value of the index varies. Mainly tourmaline, rarely also zircon or rutile, are dominating in groups A, B and E and the relative occurrence of all three minerals is quite high. It can be explained by the quite “equivalent” importance of magmatic/granitic, “high” as well as “medium” grade metamorphic rocks in the provenance area. Tourmaline and rutile dominate over zircon in group C, which can be explained by a significant role of metamorphic rocks. Similarly as in group F tourmaline dominates in group D, and the amount of zircon and rutile is reduced. It can be explained by the prevalent role (or absolute dominance for group F) of lower-grade metamorphic rocks in the source area. A different provenance (Moravian zone) is confirmed for outcrops 31 and 32 then for the rest of the studied localities (1-30). The existence of at least two parts of fluvial systems with different drainage/provenance is supposed also due to the areal position of the outcrops. A possible confluence is uncertain.

Significant similarities in the heavy mineral assemblages between the deposits of the Klikov Formation (Upper Cretaceous, South Bohemian Basins) and the SMFF (especially for groups A, B, C and E) are observed. Slánská (1967) recognised the important portions of zircon, tourmaline, rutile, kyanite, anatase and opaque minerals within the sandstones of the Klikov Formation. Also the occurrence of andalusite and sillimanite is remarkable there. A possible reworking from the rocks of the Klikov Formation is supposed but difficult to evaluate clearly, because the prime source of the deposits of the Klikov Formation were also similar crystalline rocks of the Moldanubian zone and the South Bohemian Batholith.

5. 4. 2 Zircon studies

The evaluation of the outer morphology/shape of zircon can be used for the determination of its source rocks. The euhedral shape of zircons in deposits is often considered to indicate a first-cycle detritus and the evidence of its magmatic or volcanic origin (Poldervaart, 1950; Lihou and Mange-Rajetzky,

1996). Rounded zircon grains are explained to be detrital with polycyclic history (for exceptions see Mader, 1980; Winter, 1981). In the SMFF subrounded and rounded zircons generally are the major constituents in all studied samples forming 49.0 - 72.2%. Subhedral zircons constitute between 17.4% and 40.0%. The portion of euhedral zircons generally is low - between 3.0 - 17.0 % (Fig. 8). A higher portion of euhedral zircons was recognised in the outcrops in the west, whereas a low percentage occurs in some outcrops in the middle part (outcrops 14, 17, 18) and especially in the south (outcrop 31).

The colour of zircons is ultimately linked to their age and/or abundance of radioactive elements in the crystal lattice (Pettijohn et al., 1987). Colourless zircons dominate in all samples forming 42 - 78.7% of the spectra. Zircons with pale colour shade constitute 19.7 - 44.0%. Zircons with brown colour form 3.5 - 21.2% and opaque ones 0 - 8.8%. Pink zircons are very rare (0 - 2.6%). The occurrence of opaque and brown zircons is generally higher in the eastern and southeastern part of the studied area.

The proportions of zoned zircons vary between 2 and 33.3% and older cores occur in zircons in amounts between 1 to 15.2%. A higher occurrence of zoning and older cores in zircon can be recognised in samples from the western and northern part of the studied area. The studied zircons show a high proportion of grains with inclusions. Such grains form 93 to 100% of the population.

The study of elongation (the relation of length to width of the crystals) of zircons can help to trace back the source of deposits (Poldervaart, 1950; Zimmerle, 1979; Winter, 1981). Elongation of zircons in granitoids is a function of their crystallization temperature (Pupin, 1980). The average value of elongation varies between 2.05 and 2.89. Histograms of elongation are presented in Fig. 8. Zircons with elongation between 2 and 3 dominate in the majority of the studied outcrops. Zircons with elongation between 1 and 2 only prevail in outcrops 5, 9, and 24. More than 66% of zircons with elongation higher than 2 were recognised in outcrops 1, 2, 4, 12, 14, 18, 19, and 21. Zircons with an elongation of more than 3 are supposed to reflect magmatic/volcanic origin (Zimmerle, 1979) and/or only limited transport. The presence of such zircons varied in the studied samples between 4.4 and 40.0%. A higher content of these zircons (over 20%) was recognised in outcrops 5, 12, 14, 19, and 21. Low contents (less than 10%) of highly elongated zircons were recognised in outcrops 1, 3, 9, and 17.

Zircon typology can provide data about the condition during the crystallization, i.e. about the parental magma. A different zircon typology of various magmatic chambers can be supposed, which can be used for tracing a precise provenance (Pupin, 1980, 1985; Finger and Haunschmid, 1988; etc.). No significant regional differences in typology of zircon of the SMFF were recognised. The parental magmas of the studied zircons had a hybrid character according to the position of the “typology mean point” (Pupin, 1980, 1985). Some sourced magmas were influenced by crustal material, other ones reveal a proximity to the mantle source. A dominance of two main typological subpopulations (Fig. 9) can be followed within the zircons of the SMFF. The first one is typical for the S24 subtype of Pupin (1980), whereas the second one has a domi-

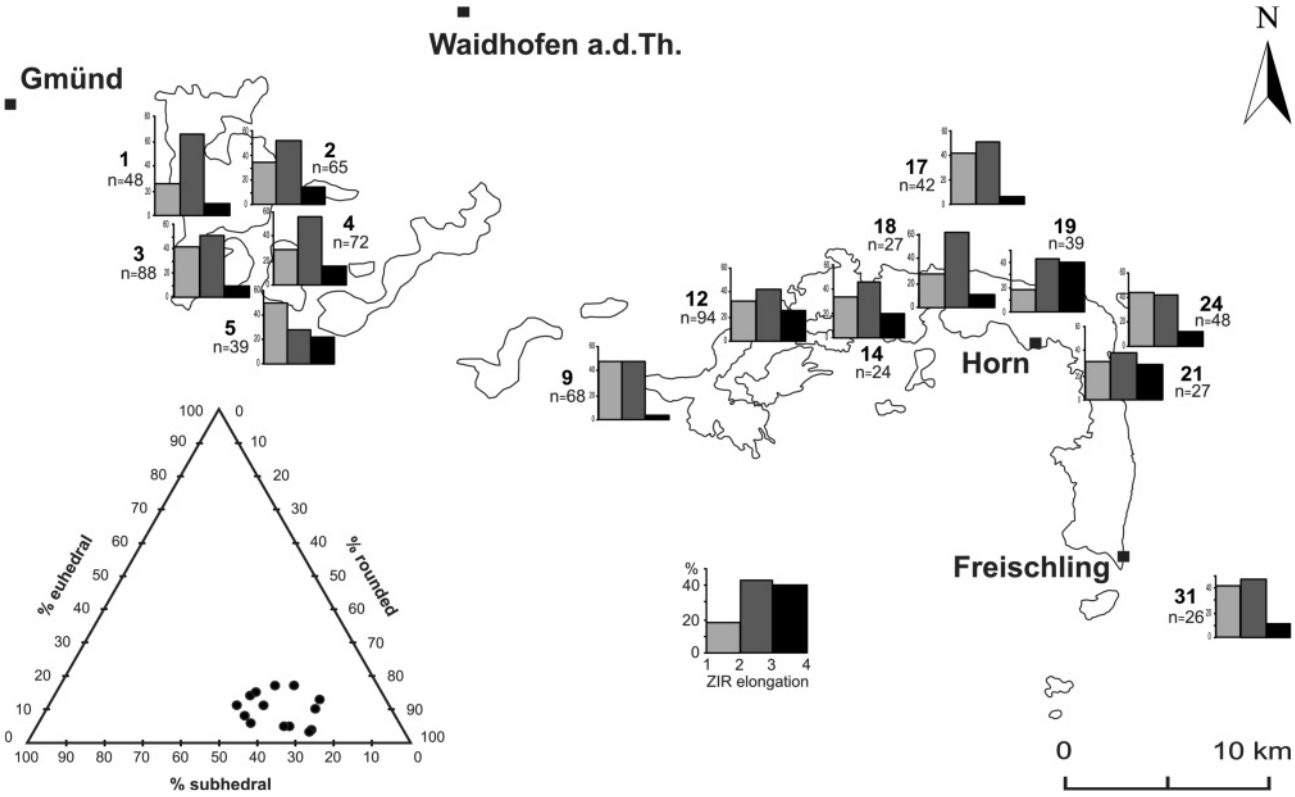

Figure 8: Elongation of zircons (707 measurements) and ternary diagram of the shape of zircons from sands of the SMFF. For position of the outcrops refer to Fig. 2.

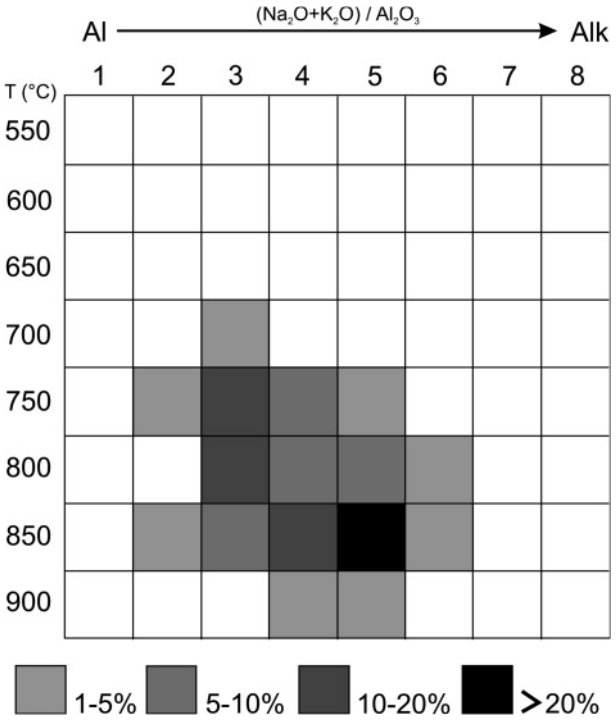

Figure 9: Typology of zircons based on 348 crystals from sands of the SMFF (14 localities) in the Pupin-diagram (Pupin, 1980).

nance of S12+S17 subtypes of Pupin (1980).

Interpretation: The results of zircon study can be interpreted as an evidence of the mixed provenance with a remarkable factor of local sources. Euhedral and subhedral zircons were dominantly derived from granitoids of the South Bohemian Batholith. Several authors proved the hybrid character of the magmas of the South Bohemian Batholith (Finger et al. 1987; Finger and Haunschmid, 1988; etc.). The rounded zircons may originate from earlier sediments (recycled detritus), from metamorphic rocks (first-cycle detritus) or even from magmatic rocks (sedimentary protolith or effects of magmatic resorption). The principal source of zircons from the South Bohemian Batholith can be deduced (see Finger and Haunschmid, 1988; Finger et al., 1991) for outcrops 1, 2, 4, 12, 14, 18, 19, and 21. A more important role of metamorphics in zircon provenance is supposed for the localities 3, 5, 9, 17, 24, and 31. Niedermayr (1967) documented an elongation of zircons for the Gföhl gneiss between 1.8 and 2.3 and for the granulites of St. Leonhard between 1.5 and 1.7. Hoppe (1966) revealed an elongation in the granulites of St. Leonhard of about 2. Humer (2003) showed that the elongation of zircons from Eisgarn granite is dominantly between 2 to 3.

A part of the studied magmatic zircons originated from the Rastenberg granodiorite where Klötzli and Parrish (1996) identified a dominance of the S 24 subtype. The zircons from this pluton are colourless to slightly pink, often with older cores; both inclusions and zonation are abundant and their mean elongation is 3:1. More complicated is the tracing of the source for zircons with a dominance of S12+S17 subtypes. The source from the Weinsberg granite is problematic because Finger and Haunschmid (1988) and Finger et al. (1987) described S2, S3, S7 and S8 subtypes as the characteristic ones. Similarly Klötzli et al. (2001) described a distinct typology L2 to S5 and S23 to D for this granite. Such a combination of subtypes relatively rarely was recognised in the zircons of the SMFF. Another possibility as source could be the Eisgarn granite. Some data about zircon shape of this granite (Finger et al., 1987) are in coincidence with results from the SMFF. According to Humer (2003) the subtype S12 is typical for Eisgarn granites, but further typical "Eisgarn" subtypes such as S1, S2, L1 or L2 were not recognised in the SMFF. A partial source is also possible from the Karlstift granite where subtypes S24, S25, S19 and S20 dominate (Humer, 2003).

5. 4. 3 Garnet

The chemistry of detrital garnet is useful and widely used for provenance determination (Morton, 1991). Results are presented in Fig. 10. The dominance of almandine is evident, but some garnets reveal a dominance of grossular, spessartine and pyrope component. Generally two areas with different garnet composition were recognised. The first one is represented by the outcrops 31 and 32, whereas all other studied outcrops form the second distribution area (Fig. 10). Garnets from outcrops 10, 11 and 17 reveal wider spectra of garnet components, a lower content of almandine and a slightly higher content of andradite and uvarovite. Garnets from outcrops 31 and 32 are generally lower in pyrope ($Mg2^{+}$) content and are relatively more uniform.

Interpretation: The data reveal a dominant garnet provenance from gneisses, (amphibole+biotite) schists and granulites. Some garnets can also originate from calc-silicate rocks or marbles, especially garnets in outcrops 31 and 32. A partial source of garnets from eclogites or more "basic" metamorphic rocks for all the other studied localities of the SMFF can be supposed.

5. 4. 4 Rutile

Rutile represents one of the most stable heavy minerals. It primarily appears in medium- to high-grade metamorphic rocks and clastic sediments. Although the preservation of information from previous metamorphic cycles in rutile is discussed (Stendal et al., 2006; Meinhold et al., 2008) the mineral is used for provenance analysis (Force, 1980; Zack et al., 2004a; Triebold et al., 2007). The concentration of the main diagnostic elements (Fe, Nb, Cr and Zr) highly varies. Some differences can be recognised between the data from outcrops 2, 5, 6, 10, 11, 14, 17, 18 and 21 comparing to data from outcrops 31 and 32.

Data from the first group of outcrops reveal 26.7% of rutile <1000 ppm Fe, an average concentration of Nb of 1739 ppm, of Cr of 525 ppm, of Zr of 1084 ppm and the value of logCr/Nb mostly is negative (84,4%). Data from the outcrops 31 and 32 reveal 54.5% of rutile <1000 ppm Fe, the average concentration of Nb is 966 ppm, of Cr 709 ppm, of Zr 1075 ppm and the value of logCr/Nb mostly is negative (72.7%).

Interpretation: The results provide the evidence of a dominant provenance of rutile from metamafic rocks (eclogites,

mafic granulites). The metamorphic temperature (Zack et al., 2004b) can be evaluated of about 880 °C (granulite facies). About 11.1 to 18.2% of rutile can originate from metamafic rocks (eclogites, mafic granulites) and about 18.2 to 24.4% of rutile can originate from amphibolites.

5. 4. 5 Monazite, spinel and tourmaline

From monazite, spinel and tourmaline only a relative low number of grains were analysed. For this reason and because of a possible scattering of the data (Pober and Faupl, 1988; Eynatten and Gaupp, 1999; Triebold et al., 2007) the presented results have only limited significance for the provenance from crystalline rocks.

The ratio of La/Nd in monazite is provenance-sensitive (Morton, 1991). In the studied samples this ratio varies between 0.96 to 1.44 (average value 1.23), which can be interpreted as an evidence of derivation from granitic rocks.

The results of monazite microprobe analysis were further used for its „chemical dating“ (CHIME) based on the content of U, Th and Pb (Parrish, 1990; Montel et al., 1996). Two populations of monazite can be recognised with an average age of 303±15 Ma and 319±13 Ma. Such a Carboniferous (Namurian-Westphalian) age confirms its provenance from the South Bohemian Batholith. A transport of material from the west (from the South Bohemian Batholith) to the east also can be proven by outcrop 24 because here the crystalline basement is formed by metamorphic rocks of the Moravian zone.

A more detailed source location within the South Bohemian Batholith by these monazite data is difficult due to controversial geochronological data from different granites from this pluton (Klötzli et al., 1999). The published ages of the Rastenberg granodiorite vary between 323-353 Ma (Friedl et al., 1992; Klötzli, 1993; Klötzli and Parrish, 1996). For the Weinsberg granite published geochronological data vary between 321-358 Ma (Klötzli, 1993; Klötzli et al., 2001). Single grain data from zircon and monazite concentrate between 328-336 Ma (Finger and v. Quadt, 1992) and 323-331 Ma respectively (Gerdes et al., 2003). Geochronological data for the Eisgarn granite lay around 328 Ma, which are slightly younger than the Weinsberg granite data (Klötzli et al., 1999; Gerdes et al., 1998, 2003). Some fine-grained granites, which intruded into the older granites, e.g. the Weinsberg granite, reveal ages between 315 to 319 Ma and monazites from the Freistadt granodiorite show ages of about 300-310 Ma (Gerdes et al., 2003). In contrast monazites of metamorphic units like from the Ostrong unit east of the South Bohemian Batholith give ages of around 335 Ma (Gerdes et al., 2006).

The microprobe study reveals broader spectra of source rocks of spinels. Some spinels (outcrops 2, 5, 6, 10, 14, 18) have a high content of Cr (2520-6290 ppm) and can be classified as chromian spinels (cf. Fig. 11). Chromian spinel is a typical mineral for peridotites and basalts (Pober and Faupl, 1988) and its presence in the heavy mineral spectra of the SMFF points to ultramafic rocks in the source area. The small gabbro massifs northeast of Schrems and/or garnet-pyroxenic amphibolites, granulites and Wolfshof syenitic gneiss in the surroundings of St.Leonhard am Hornerwald can represent possible sources of these spinels.

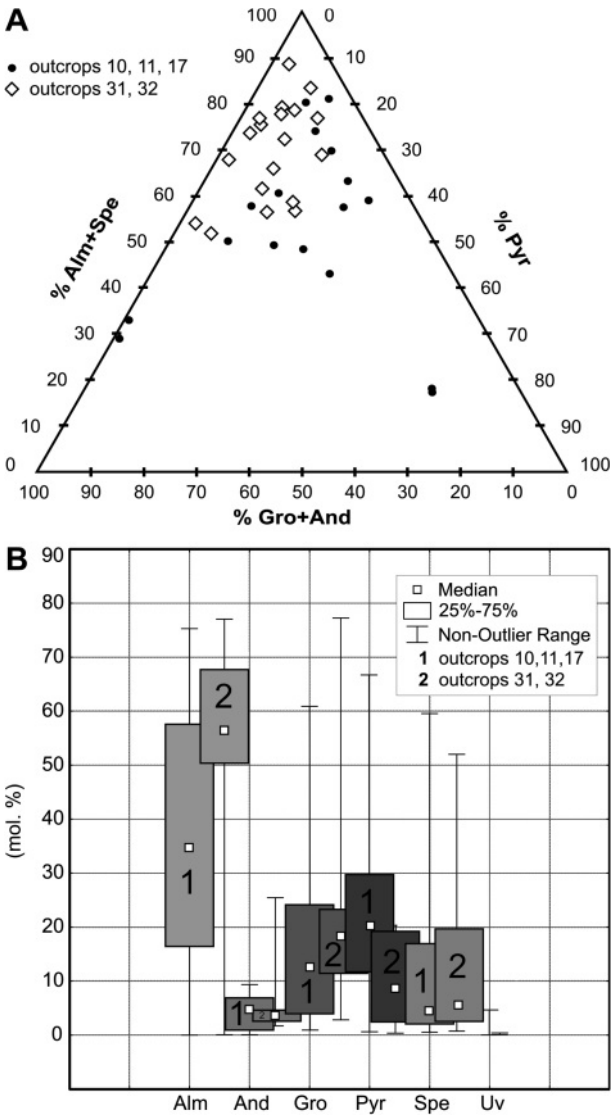

Figure 10: (A) Ternary diagram of the chemistry of detrital garnets (Morton, 1991) and (B) comparison of the chemical composition of garnets from sands of the SMFF.

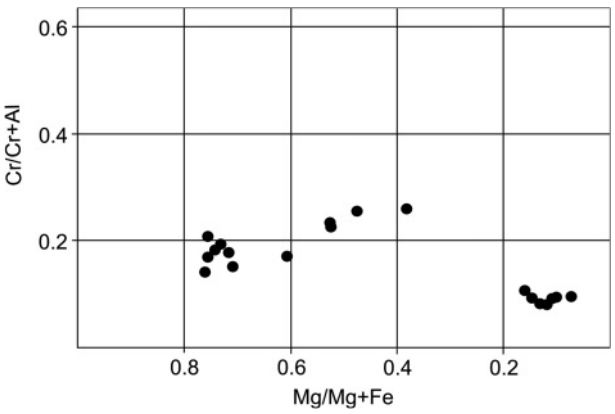

Figure 11: Analyses of spinel of the SMFF in the Cr/(Cr+Al) vs. Mg/(Mg+Fe^{2+}) diagram according to Pober and Faupl (1988).

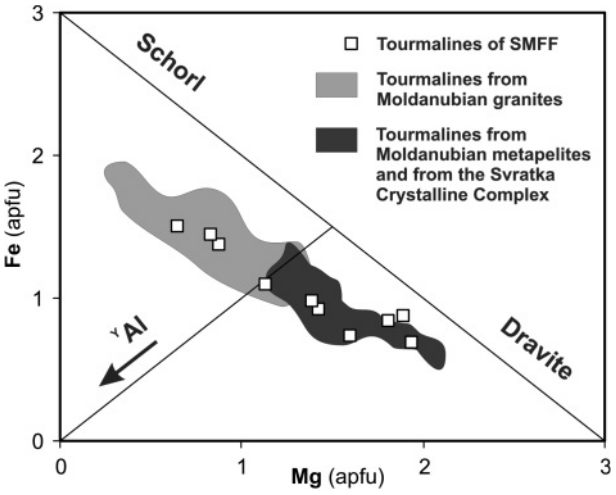

Figure 12: The chemical composition of tourmalines from sands of the SMFF in comparison with tourmalines from Moldanubian granites, Moldanubian metapelites and from the Svratka Crystalline Complex (apfu – atom per formula unit). For references see text.

Tourmalines can be classified as schorl-dravite and Al-schorl-dravite (Fe/(Fe+Mg) (= 0.26-0.70 a Al = 6.05-6.78 apfu) (Fig. 12). The chemical composition of approximately one third of the studied grains can be compared with tourmalines from tourmaline granites of the Moldanubian zone (Al rich schorls with dominance of Na in X position). Small granite bodies related to durbachites (like the Rastenberg or Třebíč pluton) can be correlated. Another third of tourmalines may originate from metapelites (dravites with dominance of Na in X position). Results from tourmaline of Moldanubian metapelites and Svratka Crystalline Complex were used for comparison (data of D. Buriánek - Czech Geological Survey, Brno). Some studied tourmaline grains reveal a higher content of Ca in X position (0.22-0.35 apfu). Such tourmalines can originate from calc-silicate rocks or marbles.

6. Depositional environment and processes

Sedimentary facies are considered to be the basic 'building blocks' of the sedimentary succession (Harms et al., 1975; Walker, 1984). The lithofacies within the studied outcrops of the SMFF were defined according to their grain size and sedimentary structures (cf. Tab. 2). The used codes conform to the standard lithofacies types of Miall (1978) improved by Bridge (1993). Lithofacies have been the basis for an interpretation of the various modes of sediment deposition. They have been combined, based on their spatial grouping and depositional architecture, into facies associations (Reading, 1996). A facies association is defined as an assemblage of spatially and genetically related facies representing a particular morphodynamic style of sedimentation, involving specific facies, bed geometries and depositional architecture (Miall, 1989; Nemec, 2005). In fluvial settings distinctive lithofacies associations are traditionally assigned as architectural elements (Miall, 1985; Bridge, 1993).

6. 1 Lithofacies

Three lithofacies groups, i.e. gravelly, sandy and fine-grained ones can be separated within the studied deposits of SMFF. The areal distribution of these lithofacies groups is presented in Fig. 13. The strongly varying vertical and lateral extent of the profiles in different outcrops could influence the results presented in this figure. Schematic lithostratigraphic logs of selected outcrops are presented in Fig. 14 and examples of selected lithofacies in Fig. 15.

6. 1. 1 Gravelly lithofacies

The gravelly lithofacies represent 59.5% of the logged profiles. Two distinct gravelly lithofacies (Gm, Gcs) were recognised.

Facies Gm

The facies is represented by massive to crudely horizontally stratified gravel and forms about 6.5% of the studied logs (Fig. 15a, c). Beds have tabular, lenticular or wedge shape and their thickness varies between 5 and 50 cm. They can be laterally traced on the distance of several meters. Sharp erosive base is typical, whereas convex up bases are rare. The upper boundary is sharp, convex up, and sometimes with scattered outsized pebbles.

The gravels are usually clast-supported, rarely clast- to matrix-supported. Openwork fabric is rare. Very coarse sand with granules usually forms the matrix. Pebble clusters were observed in several outcrops. The preferred orientation of pebbles is poorly defined, if developed then both A(t), B(i) and A(p), A(i) imbrication could be found (Walker, 1975).

The diameter of the maximum clast varies in various beds/outcrops between 3 and 20 cm. The pebbles usually are subrounded to subangular, but also angular or well rounded ones were recognised. Muddy intraclasts sometimes were observed. These usually were markedly larger than extraclasts, with max. 25 cm in diameter. Their presence seems to be lower within Gm beds than in Gcs beds. Large (about 1 m in diameter) fragments of trunks and stems, formally rafted, were observed in several outcrops.

Interpretation: Horizontal stratification and poorly developed imbrication suggest rapid deposition from low-density tractional bedload. The facies represents the coarsest and least mobile bed-load material, deposited after erosional stage as a response of diminishing of the peak flood as a low-relief migrating gravel sheet. Such a deposition typically happens in pulses and very rapidly (Reid and Frostick, 1987; Whiting et al., 1988). Bedload sheets form on bar surfaces and in channels at flow velocities just above the threshold of gravel motion. They are transitional bedforms that can develope into gravel dunes. Imbricated grains and pebble clusters occur in the relatively immobile bedload of the trough and lower stoss sides of the bedload sheets, whereas smaller and more mobile gravel grains are moved on the bedform crests (Lunt et al., 2004). Clasts derive both from the drainage area, banks and overbank deposits (Hein, 1984; Nemec and Postma, 1993). The facies forms internal/initial parts of the gravel bar (bar core) or channel lag.

Facies Gcs

This facies is formed by cross-stratified gravel or sandy gra-

Lithofacies	Lithology and sedimentary structures	Interpretation
Gravelly lithofacies (G)		
Gm	Gravel. Massive or crudely horizontally bedded, imbrication.	Internal parts of longitudinal bars, lag deposits. Deposition from migrating bedload sheets.
Gcs	Gravel or sandy gravel. Trough, planar and low-angle cross-bedding.	Mid-channel dunes and bars. Growths from older bar remnants. Minor channel fills.
Sandy lithofacies (S)		
Sp	Sand, fine to very coarse, sometimes pebbly. Solitary or grouped planar cross-bedding.	Lingoid and transverse (inner) bars and dunes (straight-crested), sand waves (lower flow regime), final stages of channel filling.
St	•Sand, fine to very coarse, sometimes pebbly. Solitary or grouped trough cross-bedding.	Channel deposits, curved-crested bars or dunes, crevasse-splays.
Sh	Sand, very fine to very coarse. Horizontal lamination or bedding, parting lineation.	Planar bed flow (lower and upper flow regime), top bar deposits, channel filling.
Sr	Sand, very fine to coarse. Ripple marks and ripple cross-bedding.	Final stages of minor channel infilling, top parts of channel bars or crevasse-splays.
Sm	•Sand, fine to coarse. Massive	Top parts of channel bars
Fine-grained lithofacies (F)		
Fm	Clay, silt. Massive.	Overbank deposits, channel fill or drape deposits.
Fh	Clay, silt. Horizontal lamination.	Abandoned channel fills, levee, overbank deposits.
Fr	Very fine sand, silt. Rootlets.	Vegetated overbank deposits. Seat earth, soils.

Table 2: Lithofacies types of the St. Marein-Freischling Formation and their interpretation (Lithofacies code of Miall, 1996).

vel and can be subdivided into planar and trough cross-stratified subfacies (Fig. 15b, c, d). The quality of outcrops did not always allow distinguishing between these subfacies. Facies Gcs forms about 53.2% of the logged profiles. Beds have wedge, lenticular or channel like shape and their thickness varies between 6 and 100 cm. They can be laterally traced on the distance of about 3 m. Beds are often stacked upon one another into bedsets, which can be up to 3 m thick (mostly about 1 m). An upward reduction of both bed thickness and grain size can be followed in such stacked bedsets. Sharp erosive base with scoured or undulated shape is very typical. A relief of more than 1 m on the horizontal distance of 3 m was traced along the base. Convex-up base is rare whereas convex-up top is very typical. The upper bed boundary also is erosive, concave, undulatory or inclined, sometimes with scattered larger pebbles.

Gravels are usually clast supported, rarely clast to matrix supported. An openwork fabric was recognised very rarely. Very coarse to coarse sand or granules form the matrix. Alternation of more gravelly and more sandy layers/laminas, occurrence of clast supported lower parts of the beds in contrast to matrix supported upper parts, upward reduction of the gravel content, and increase of the content of sand and granules were all observed. The inclination of cross-strata is generally relatively flat (dip-angle about 10°) and varies between 5-30°. Both angular and tangential foresets were observed, sigmoidal shape is rare. A preferred orientation of pebbles is common. The imbrication of A(t), B(i) type dominates but also A(p), A(i) type was recognised.

The diameter of the maximum clast varies in individual outcrops between 1 and 10 cm. The largest pebbles usually were located along the base of the bed or reactivation surface. Pebbles are usually subrounded to subangular, but also well rounded ones can be found. The presence of muddy intraclasts (diameter from 2 up to 20 cm) is typical. Intraclasts are usually larger than extraclasts if compared within the same bed. Large fragments of trunks and stems (about 70 cm in diameter) sometimes were located along the base of a bed. Maximally 10 cm thick discontinuous interbeds of facies Sp follow within thicker units of facies Gcs.

Interpretation: Facies Gcs is a product of deposition from steady traction flows, formed by foreset deposition along an avalanche face at the downstream end of a bedform (Kostic and Aigner, 2007). This facies can be classified as medium-scale cross-stratification (Lunt et al., 2004). That is formed by sinuous-crested dunes and represents the most common internal structure of bars and channel fills. The mean set thickness is related to the mean height of formative dunes. Cross-sets that are 0.1-0.4 m thick typically would be formed by dunes with mean heights between 0.3 and 1.2 m. Higher dunes occur in deeper parts of the channel (Lunt et al., 2004).

The scour-bounded, fining-upward composite units of superimposed Gcs beds are thought to be channel-fill deposits of a powerful bedload stream (braided river?). Larger pebbles scattered along the upper bed boundary reflect later reworking (during the lower stage of fluvial discharge). Thin discontinuous sandy interbeds are erosional relics. The stratification defined by contrasting grain sizes or lateral and vertical reduction of the grain size may reflect changing water stages over the flood cycles, temporal variations in flow strength (Smith, 1974; Ramos and Sopeńa, 1983; Rust, 1984), clast segregation over the surface of the bar (Steel and Thompson, 1983), or migration of smaller bed forms over dune/bar crests (Rust, 1984; Miall, 1996; Lunt et al., 2004). The low-angle stratification and lithofacies assemblages could suggest that the gravel was transported partly as bedload sheets (Hein and Walker, 1977).

6. 1. 2 Sandy lithofacies

The sandy lithofacies represents 31.5 % of the logged profiles. Five distinct sandy lithofacies (Sp, St, Sh, Sr, and Sm) can be recognised.

Facies Sp

This facies is represented by planar cross-stratified sands and forms 16.8 % of the logged profiles. A channel-like, wedge or tabular shape of beds is typical. The thickness of the beds varies between 15 and 70 cm. Stacked bedsets of facies Sp can reach up to 200 cm in thickness. The soles usually are erosive and scoured, but flat, convex up and undulatory ones were also observed. Loading structures along the base sometimes can be traced. The character of upper bed boundary varies, i.e. erosive, convex-up, concave, undulatory, and inclined tops were all observed.

Sands are mostly fine, medium to fine-grained, rarely coarse to very coarse, and generally quite well sorted. Scattered granules or small pebbles (up to 2 cm) or thin laminas of that grain size were rarely observed within the sands. Pebbles and muddy intraclasts (ø up to 10 cm) sometimes can be traced along the base of the beds. Pebbles can reveal imbrication of A(t) type. Remnants of wood and stems are very rare.

Both angular and tangential contacts of cross-beds can be observed, whereas the tangential forms seem to be more often developed.

Interpretation: The facies Sp is connected with foresets from avalanche faces of advancing sand dunes during lower flow regime. It was recognised within channel deposits, bars and dunes. A higher content of pebbles and granules along the base of the beds can be explained by migration of smaller bed forms over dune/bar crests providing variable supply of sediment sizes (Rust, 1984; Miall, 1996; Lunt et al., 2004). Beds of facies Sp sometimes represent erosional relics.

Facies St

The facies is represented by trough-cross-stratified sand and represents 11.1% of the studied profiles. Beds have usually lenticular or channel like shape. Wedge shape is rare. The thickness of individual sets is 10 to 20 cm and that of stacked bedsets varies between 20 and 110 cm. Several inclined reactivation surfaces were typically recognised within the thicker beds. The base usually is erosive and undulatory, whereas a convex-up shape is rare. The character of the upper bed boundary varies. Erosive, undulated or even convex up shapes

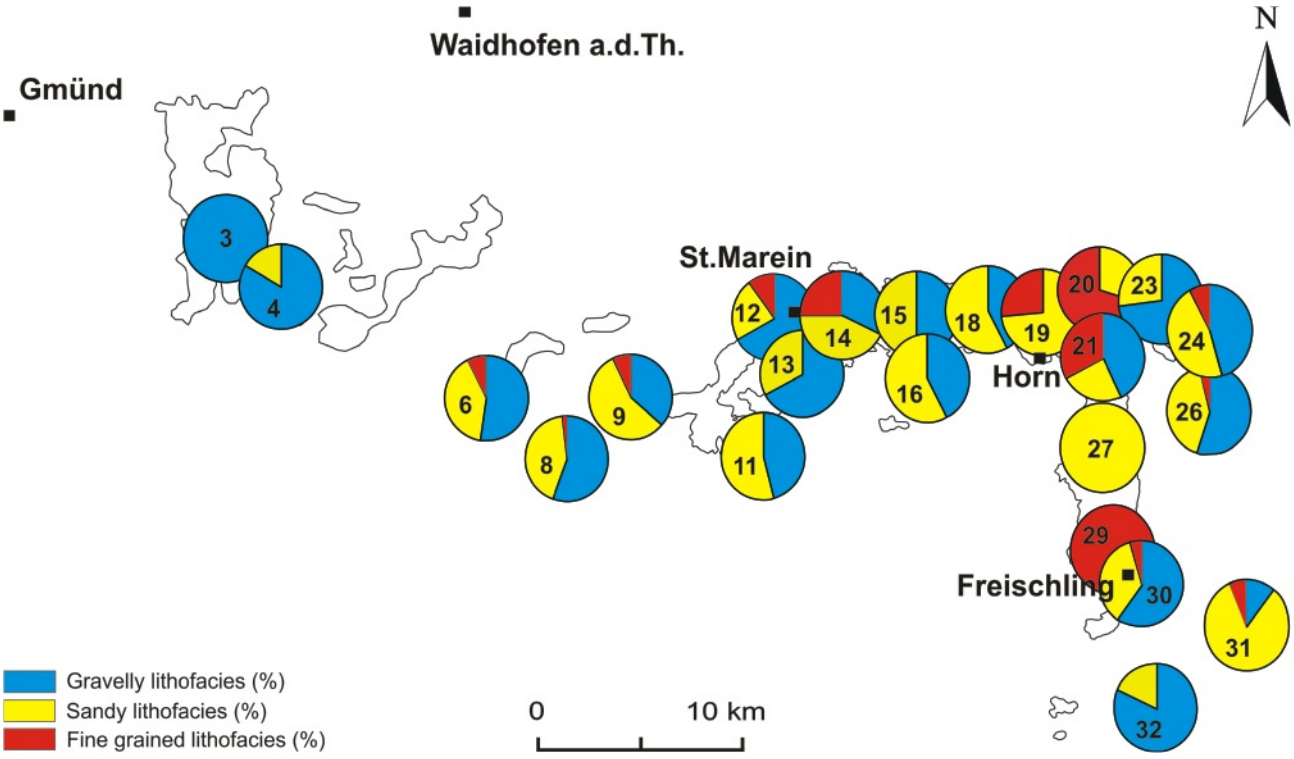

Figure 13: Distribution of the three major lithofacies groups of the SMFF. For position of the outcrops refer to Fig. 2.

were observed.

The sand often is coarse-grained, rarely very coarse or fine to medium. Laminas of granules and small pebbles or scattered small pebbles (ø up to 0.5 cm) were recognised within the sand. Upward fining of average grain size can be followed within the thicker beds. Occurrence of granules and coarse sand is more abundant close to the base. Fine to medium sand predominates to the top.

Interpretation: Facies St is interpreted as a product of deposition from traction flows during lower flow regime. It can be connected with the migration of 3D dunes, infill of minor channels (observed width 50-120 cm) or depressions (cut and fill). The gradual fining upward suggests a gradual diminution of the flow and filling of the channels.

Facies Sh

This facies is represented by horizontally laminated sand and forms only 2.4% of the logged profiles (Fig. 15e). Beds have tabular or wedge shape and their thickness varies between 5 and 80 cm. Convex up, convex down and also undulatory bases were observed. A scoured sole has a relief of more than 1 m on the distance of 4 meters. The top is erosive and undulated.

Grain size varies from very fine to coarse with admixture of granules. Discontinuous laminas of mudstone (deformed by loading) were also observed within the beds of facies Sh.

Interpretation: The deposition from traction flows near the transition phase between lower and upper flow regime is responsible for the deposition of this facies. Unsteady flow conditions and rapid changes in flow dynamics are supposed. The portion of deposition from suspension is reflected by muddy laminas. The heterolitic structure indicates varying hydrodynamic conditions during deposition. The multiphase origin can be related to successive channel abandonment. The facies can be related to final stages of the channel filling, washed out phases over the top of the bar/dune, formation of sand flats, and aggradation on a plane or low-angle bed in peripheral areas of the channels or flats.

Facies Sr

The facies is represented by ripple cross-stratified sand and forms only 0.9% of the studied profiles (Fig. 15e, f). Beds have tabular or lenticular shape and often represent only erosive relics. Their thickness varies between 5 and 30 cm. Soles are mostly flat and rarely gradational. Tops are usually eroded.

Very fine to coarse-grained sands, which are usually well sorted, form the facies Sr. An admixture of small intraclasts (ø up to 1 cm) is very rare. Various kinds of current ripples, including climbing ripples, are observed.

Interpretation: The facies is interpreted as a product of deposition from waning traction flows in the lower flow regime. Ripples form during low-flow stage or during floods in areas of slow-moving water. Small-scale cross-strata are generally associated with the deposition in channels (final stages of the minor channel infilling), bar-tails, troughs and crests of dunes (Lunt et al., 2004).

Facies Sm

This facies is formed by massive sand and was recognised in only 0.3 % of the studied profiles. Beds of lensoidal shape laterally are pinching out on a distance of less than 3 m. Their thickness varies between 6 and 20 cm.

The sole is sharp and undulated with a relief of several centimeters. The top is erosive. The sand is poorly sorted, fine to medium, in rare cases even coarse-grained, with some admixture of both silt and scattered small pebbles (ø max. 3 cm).

Interpretation: Facies Sm appears only as erosional remnants within the beds of facies Gcs. Spatial relation to the gravelly facies reflects the formation of sandy interbeds within the gravelly beds. It can be interpreted as waning stage of the formation of gravel bars. During the reduced channel discharge, bar movement stopped and occasional sandy deposition could be connected with the overflow (crossover channels, sandy sheets, dunes). Some portion of deposition from suspension on bar platforms can be supposed (see fine-grained lithofacies).

6. 1. 3 Fine-grained lithofacies

The fine-grained lithofacies represent 9% of the logged profiles. Three distinct fine-grained lithofacies (Fm, Fh and Fr) were recognised and typically comprise clay and silt-size grains.

Facies Fm

Structurless (massive) mudstone represents the facies Fm, which is the most abundant fine-grained facies in the studied deposits of the SMFF forming 4.5% of the logged profiles. The thickness of the beds laterally is very unstable, and it varies between 5 and 150 cm. Differences of several decimeters in thickness were observed on the distance of 2 meters. The facies often is present only as erosional relic, usually as a drape on a gravel deposit (Fig. 15h). The base is very irregular with concave or undulated shape. The top is typically sharp and erosional; small loading structures were observed rarely.

The mudstone is formed by light grey to whitish grey, dark brown, olive green, or greenish grey sandy clay-silt or sandy silt-clay (Fig. 4a, b). Laminas of very fine to fine sand sometimes were observed, usually along the base of the bed of facies Fm. Discontinuous laminas of granules or small pebbles exceptionally were recognised within the mudstone.

Interpretation: This facies is interpreted as a product of deposition from suspension during waning flow conditions. A rarely recognised heterolitic structure indicates varying hydrodynamic conditions during deposition. Fine sandy laminas are interpreted as deposits of weak traction currents. Fining-upward sequences may represent a single flood (Lunt et al., 2004). Suspended material settled out rapidly in abandoned channels.

Facies Fh

Horizontally laminated mudstone forms facies Fh and represents only 4.1% of the logged profiles (Fig. 15g). The thickness of beds highly varies from 2 cm up to 150 cm. The facies was recognised either as several centimeters thick and several meters extended discontinuous interbeds within gravelly facies, or as thick but laterally limited beds with a channel shape. The soles usually are sharp and slightly or highly irregular. A gradational base is exceptional. The upper bed boundary always is erosional.

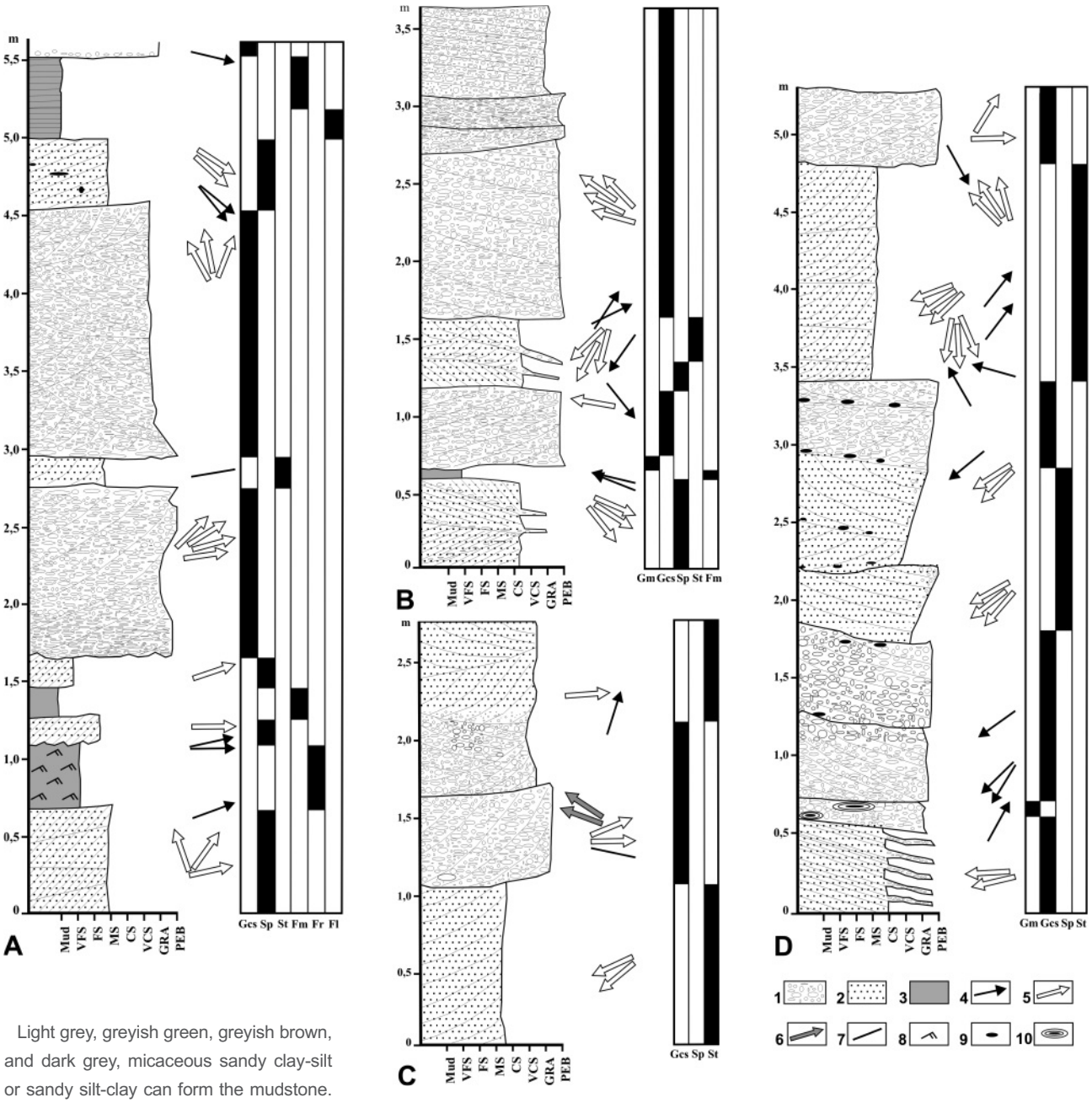

Light grey, greyish green, greyish brown, and dark grey, micaceous sandy clay-silt or sandy silt-clay can form the mudstone. Laminas of very fine sand were observed within the beds of facies Fh.

Interpretation: The facies is interpreted as a product of deposition from suspension during waning flows. Laminas of fine sand are interpreted as deposits of weak traction currents. The heterolitic structure indicates varying hydrodynamic conditions during deposition. Periodic fluxes of sediment were followed by stagnant periods. A higher content of sandy laminas sometimes can reflect transitions between facies Fh and Sh. The facies is the result of the infill of abandoned channels and is often preserved only as erosional relic.

Facies Fr

Mudstones with rootlets represent facies Fr. The facies was recognised exceptionally forming only 0.4% of the studied profiles. Beds are usually tabular in shape with thickness of about 45 cm. The base is sharp and only slightly undulated (relief in cm-range). The upper bed boundary generally is planar with loading structures.

Greyish, greyish brown and dark grey, micaceous, very fine sand to silt forms the facies Fr.

Interpretation: The facies is interpreted as a product of deposition from waning flows and suspension within abandoned channels. Later the deposits were vegetated, which reflects a longer subaerial exposure of the bed.

6. 2 Vertical facies organisation

Despite of the limitation of Markov analysis (Krumbein and Dacey, 1969; Harper, 1984) for the discrimination of the fluvial style (Brierley, 1989) we applied this method for the studied deposits for the recognition of preferential facies transitions. Although vertical organisation of small-scale sedimentary structures propose a little help for understanding large scale orga-

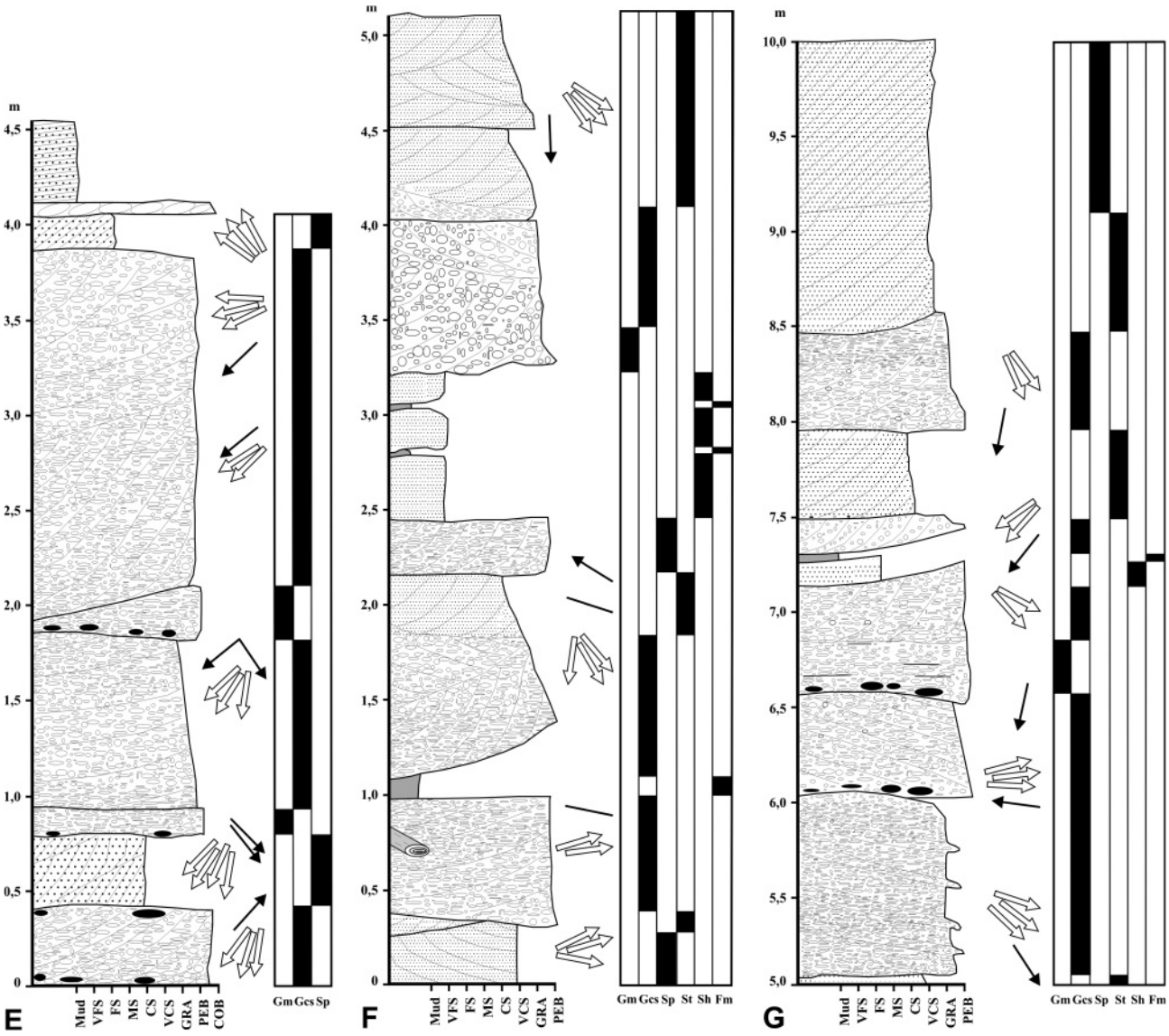

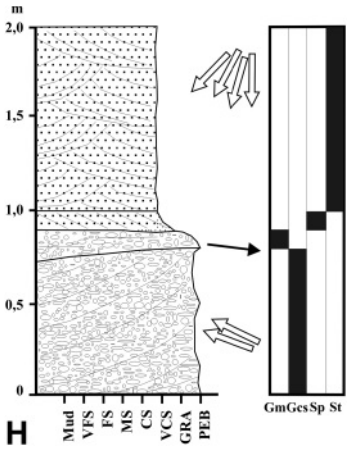

Figure 14: Schematic lithostratigraphic logs with lithofacies distribution of selected outcrops of the SMFF. A: No. 14 (Fürwald), B: No. 23 (Rodingersdorf-A), C: No. 9 (Thaures-E), D: No. 30 (Freischling), E: No. 32 (Obernholz), F: No. 12 (St. Marein - lower part of the log), G: No. 12 (St. Marein - upper part of the log), H: No. 21 (Breiteneich). For position of the outcrops refer to Fig. 2. 1: gravel, 2: sand, 3: mud, 4: direction of pebble imbrication, 5: direction of cross bedding, 6: direction of channel axis, 7: bounding surfaces direction, 8: ripples, 9: muddy intraclasts, 10: trunk fragments.

nisation, this method additionally offers the possibility to combine data from varied outcrops and evaluates the reliability of the proposed facies associations.

The upward transition from facies Gm to facies Gcs was most clearly recognised (d = 0.5) and can be explained by gravel bedform migration (Siegenthaler and Huggenberger, 1993; Lunt et al., 2004; Kostic and Aigner, 2007) (Fig. 15c). It further can be prolonged into a two step facies transition Gm-Gcs-Sp (d = 0.2). This cyclic fining upward interval reflects flood events and the accretion of midchannel bars. The lateral alternation of facies Gcs with Gm and the sandstone lithofacies are also explained as variations in gravel sheet growth (Hein and Walker, 1977).

The recognised one step facies transition Gcs-St (d = 0.3) reflects processes in concave–up scours. The one step transition Sr-St (d = 0.36) reflects the overriding of the ripples by subsequent sandy dunes. Such processes can be connected with bar flanks or its top. Further one step transitions Sh-Fh, Sr-Fh, Fh-Fm, and Fh-Gm (d between 0.12 and 0.23) reflect processes in the abandoned channels (alternation of stagnant and active flow periods, erosion during the subsequent flood event).

The results of the Markov analysis can be compared with the relative abundance of the selected facies. The most abundant facies, i.e. Gcs,

Sp, St and Gm (altogether 87.6% of the logged profiles) represent the lower/basal parts of bars and dunes. Top parts of bars and dunes are predominantly represented by facies Sh, Sr and Sm, which form only 3.3% of the studied successions. Fine-grained facies Fm, Fh and Fr (9.0 % of the logged profiles) are connected with abandoned channels. Gradual fining upward successions of gravels into sands and finally mudstones suggest the role of vertical aggradation.

6. 3 Facies associations and architectural elements

Architectural elements in outcrops are characterized by their facies associations, nature of their bounding surfaces (depositional architecture), external geometry and internal structure (Kostic and Aigner, 2007) (Fig. 16, 17). Four architectural elements have been recognised within the studied deposits of the SMFF, i.e. gravelly channel dunes and bars (GDB), channels (CH), sandy channel dunes (SD) and abandoned channels (ACH). The absolute majority of the studied outcrops was relatively small (extent of only few meters) and the logging was only possible along one outcrop wall. Insufficient outcrop conditions affected the recognition of the accurate hierarchy of bounding surfaces (Miall, 1996; Holbrook, 2001) as well as scale and geometry of selected elements. Selected architectural elements are connected with multistory fill of the channel belt.

6. 3. 1 Gravelly channel dunes and bars (GDB)

GDB represent a significant architectural element of the SMFF, which is dominantly formed by facies Gcs and Gm (Fig. 14b, c, e, f, g; Fig. 15a, b, c, d). Discontinuous thin (max. 15 cm) interbeds of sandy facies (Sh, Sp, Sm), lenses of fine-grained facies (Fm, Fh) (Fig. 15h), and bounding surfaces within the GDB element, reflect different scales of strataset superimposed upon each other. The thickness of the element GDB highly varies from about 0.4 m up to 3.5 m. A thickness of more than 0.6 m is connected with vertically stacked stratesets. The shape of element GDB dunes can be lenticular, tabular or slightly undulated and generally resembles sheet like bodies often influenced by channel geometry. The element can be laterally traced up to 20 m, but usually to a lesser extent than that. Scoured erosive base and convex up top are typical. Planar horizontal lower boundary rarely was recognised. Further selected architectural elements locally interfinger with GDB, commonly occur on the top of it and are separated by a sharp contact (Fig. 17).

Interpretation: The scour-bounded, fining upward composite units are interpreted as bars of powerful bedload braided streams/rivers (Miall, 1996; Ilgar and Nemec, 2005; McLaurin and Steel, 2007). The occurrence of multiple internal bounding surfaces, textural and structural differences in adjacent sets and the presence of sandy interbeds or muddy lenses, reflect the existence of dunes on the bars surface, the formation of the bar during several depositional events, and also the possible existence of bar lobes (Lunt et al., 2004). Individual stratasets of dominantly Gcs facies are interpreted as dunes. They are separated by bounding surfaces and staked into cosets (compound dunes). Dunes are vertically and laterally stacked into bars.

Facies Gm forms the bar core which was deposited during periods of intensive sediment transport under full stage channel conditions. Bars started both to aggrade and prograde during the subsequent flow condition. The formation of cross-stratified gravel with sets and cosets of Gcs facies reflects the stage (Ramos and Sopeńa, 1983; Hein, 1984), when dunes migrate on the surfaces of bars. Dunes occur on the surfaces of most bars and in channels during high-flow stage (Lunt et al., 2004). Bars grew by accretion onto their upstream, lateral and downstream margins and filling of their swales (longitudinal, transverse and oblique bar accretion) (Nemec and Postma, 1993; Miall, 1996; Lunt et al., 2004). Lateral accretion can be connected with late stages of bar development, when vertical growth has reached some limit and the flow is diverted around the flanks (Miall, 1996). Bars may migrate downstream through barhead erosion and bar-tail deposition (Lunt et al., 2004). The thin interbeds of sandy and fine-grained lithofacies have been deposited during waning flows (Bluck, 1976). Sandy and muddy interbeds occur randomly throughout bar deposits, but are more common towards their top and downstream ends. Fining-upward trends were recognised in mid-bar, bar-tail and confluence scours (Lunt et al., 2004). Thin interbeds of mudstones can be also related to the proximal part of a overbank area. Further evidence supporting the preservation of the overbank deposits within the studied succession (levees, crevasses) is missing. Mudstones can be also connected with erosional relics of abandoned channels (see ACH element).

Large variance in the paleocurrent trends of the braid bar was described within various parts of the bar (Shukla et al., 1999), various stages of bar development (Bridge, 1993) and position (Miall, 1996). The varied shape of GDB can be with a consequence of various types of dunes and bars (longitudinal, transverse, diagonal, linquoid, etc.), erosional processes or varying orientation of the actual profile towards the paleoflow.

6. 3. 2 Channels (CH)

This element is characterized by an asymmetric channel shape with distinct erosional concave-upward base and a sharp, often flat top. CH shows internally concave-upward stratification that is predominantly parallel to the channel cross-section especially in across-stream profiles. The internal structure is commonly composed of trough-shaped cross-bed sets of predominantly Gcs, rarely St, and Sp facies (Fig. 14b, c, d, f, g; Fig. 16c, d, e, f). Close to the base the facies Gm sometimes can be recognised. Top parts can be connected with minor occurrences of Sh and Sr facies. It was possible to track the element on a lateral distance of several meters.

Interpretation: The trough-shaped cross-bedded element is interpreted as a channel-fill deposit. Sometimes near the top of GDB deposits small channel fills (up to 1 m thick) can be distinguished from larger channel fills (more than 1 m thick),

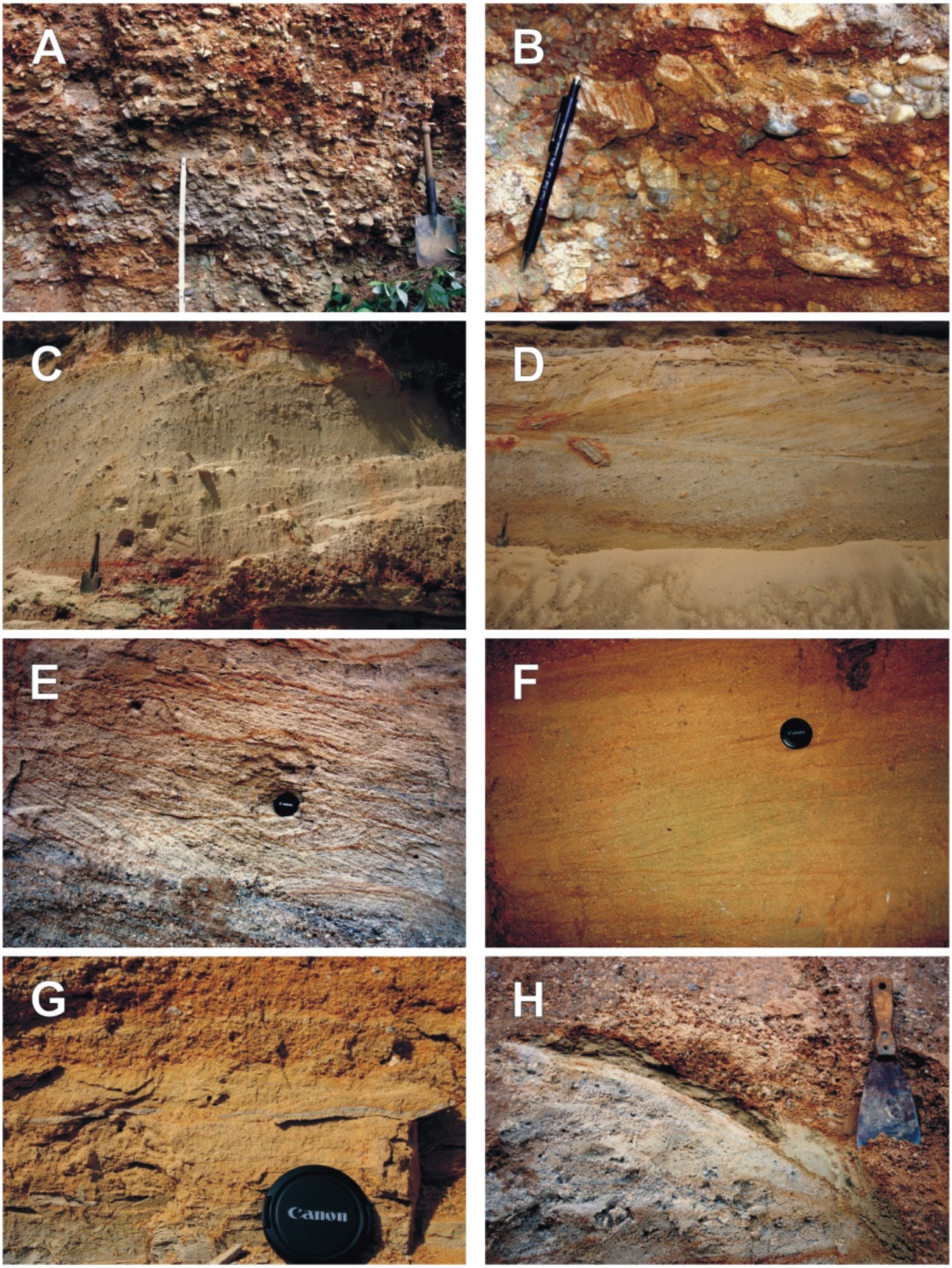

Figure 15: Structural and textural features of the studied deposits of the SMFF. A: the internal parts of the gravel bar (bar core) – lithofacies Gm (No. 11 - Altpölla), B: preferred orientation of pebbles – lithofacies Gcs (No. 4 - Mayerhöfen), C: accretion of channel bar – facies Gm (bar core) covered by facies Gcs (No. 32 - Obernholz), D: vertically stacked sets of facies Gcs – gravel dunes (No. 32 - Obernholz), E: alternation of facies Sr and Sh forming the upper part of a fluvial dune (No. 21 - Breiteneich), F: multiple repetition (coset) of facies Sr (No. 18 - Frauenhofen), G: heterolitic structure of facies Fh - channel abandoning processes (No. 12 - St. Marein), H: erosional pelitic remnants (facies Fm) within the gravelly facies Gcs (No. 12 - St. Marein). For position of the outcrops refer to Fig. 2.

which have a similar thickness as adjacent bars. Small channels are interpreted as chute or cross-bar channels that developed during floods (Lunt et al., 2004). Solitary wedge shaped sets of angle-of-repose cross-strata result from deposition of gravelly delta like lobes at the end of small channels (Bluck, 1976).

The infill of larger channels (confluence scours?) (Best, 1988; Kostic and Aigner, 2007) is not simple and several bounding surfaces – mostly third- and fourth-order surfaces of Miall (1996) – can be recognised. Shape and lateral extent of the element depend on paleoflow orientation relative to the outcrop orientation.

Coarse-grained material was transported and deposited in the deeper parts of the channels where it forms the massive infill - channel lag (Marren, 2001). Large fragments of trunks and stems were also transported in these deepest parts of the channels and locally buried in the channel lag. Sets of inclined strata deposited by bars pass laterally into channel fills or are truncated by them. The proportion of sand increases downchannel and towards the top of the channel fills (Lunt et al., 2004). Channel scour, accretion of dunes and bars can lead to changes in channel orientation resulting in complex accretionary geometries (Ramos and Sopeńa, 1983). Braided patterns (lateral shifting of the channels) provide little evidence of channel belt margins because only temporary margins of channels cut into the previous channel infill were observed in studied outcrops. Channel migration is connected with lateral erosion of bank material. So the type of channel bank material (especially cohesive one) also influences the nature of the channel fill. The recognised deposits reflect the predominance of non-cohesive sandy and gravelly banks. Such highly erodible banks are favourable for the development of generally broad and shallow channels. Scour features commonly occur at channel confluences and their forms depend on channel geometry, confluence angle, discharge, sediment load, and lateral or longitudinal shifts of the scour (Best, 1988; Ashmore 1993; Kostic and Aigner, 2007). Siegenthaler and Huggenberger (1993) proposed that the filling of scours is accomplished by: (i) foreset deposition at their upstream ends, and (ii) lateral accretion along their flank. Larger channels represent parts of the channel belt.

6. 3. 3 Sandy channel dunes (SD)

This element dominantly is formed by facies Sp and St. Less common is the occurrence of facies Gsc, Sr and Sh. Facies Sr was recognised in the upper parts of the element. The thickness of element SD highly varies from about 0.4 m up to 1.6 m. A thickness of more than 0.5 m is connected with vertically stacked dunes with several reactivation surfaces. The SD element can be laterally traced on the distance of max. several meters. Shape and thickness of the SD element is affected by the adjacent GDB elements (Fig. 14b, d; Fig. 16g, h). The shape of both bases and tops varies. It can be scoured, flat, convex up, erosive or even gradual. SD elements usually were formed directly above or laterally adjacent to the GDB element. SD elements are often eroded by successive GDB elements. SD is rarely covered by deposits of abandoned channels (ACH). Generally the SD elements are both less common and have a smaller scale than GDB and CH elements.

Interpretation: Gravel bar formation and movement stopped during reduced flow or in periods of more stabilised flows. Gravel and sand were transported over the bars as dunes giving rise to facies Gcs, Sp and St. As the river discharge fell, the top part of bars were covered by sand flats (facies Sh or Sr) or cut by numerous ephemeral/crossover channels which were filled by facies Gcs, St, Sh, Sm, and Sr connected with migration of mainly sandy dunes. These processes can modify the shape of the GDB (Ramos and Sopeńa, 1983). One or two grains thick gravel laminas within sandy beds could be connected with marginal parts of bedload sheets. SD is generally supposed to reflect the deposition within lower-order channels at lower discharge than GDB. Complex accretion (i.e. both downstream and lateral) of SD within shallow and mobile channels can be supposed. Reactivation surfaces reflect fluctuations of the flow regime, probably due to seasonal changes.

6. 3. 4 Abandoned channels (ACH)

This architectural element is dominantly formed by the facies Fm and Fh, rarely by the facies Fr. Interbeds of facies Gm, Sp, Sr, and Sh rarely were recognised (Fig. 14a; Fig. 16a, b, e, f). Interbeds of facies Gm are very thin (up to several cm), whereas interbeds of facies Sp can be up to 0.2 m thick. ACH deposits have typical asymmetric channel shape with a concave-upward lower surface and a sharp, often erosive top. The thickness highly varies from about 0.4 m up to 1.6 m and the maximum lateral extent is almost 6 m. ACH was mainly recognised in superposition of the GDB element (Fig. 16c, d). ACH represents the least common element.

Interpretation: This element is interpreted as the infill of abandoned channels. Typical bar and channel patterns formed in highly varied fluvial discharge and morphology of elevation and depression/pools is also reflected by ACH. It can suggest the periodic character of the flows. The role of channelling for both the formation of accommodation space and preservation of mudstone deposits is crucial. Subsequent rise of the flow discharge led to erosion of the abandoned channel and formation of scoured erosional top. The only evidence of quiet period and cohesive deposits is preserved as ACH and muddy intraclasts and interbeds within GDB. The frequency of channel avulsion is probably related to special climatic conditions (large magnitude floods) or connected with tectonics (Leeder, 1999).

Mudstone beds with a channel shape reflect “rapid” channel abandonment (avulsion). It can be supposed especially if mudstones are recognised directly above the gravels. Parts of the channel/channels were cut off from the main flow and quiet condition promoted the sedimentation of the finest sediment from suspension or from weaker currents (lithofacies Fh, Sh). Parts abandoned for a prolonged period of time gave rise to vegetation and soil formation. Gravelly and sandy interbeds

reflect dramatic differences in the flow discharge. They are likely to have been deposited by high floods that split from the channel and can be connected with the marginal position of the profile towards the fluvial paleochannels.

6. 4 Paleocurrent analysis

Paleocurrent data are important for the definition of architectural elements, depositional system geometry and paleodrainage analysis. The results (Fig. 18) are based on more than

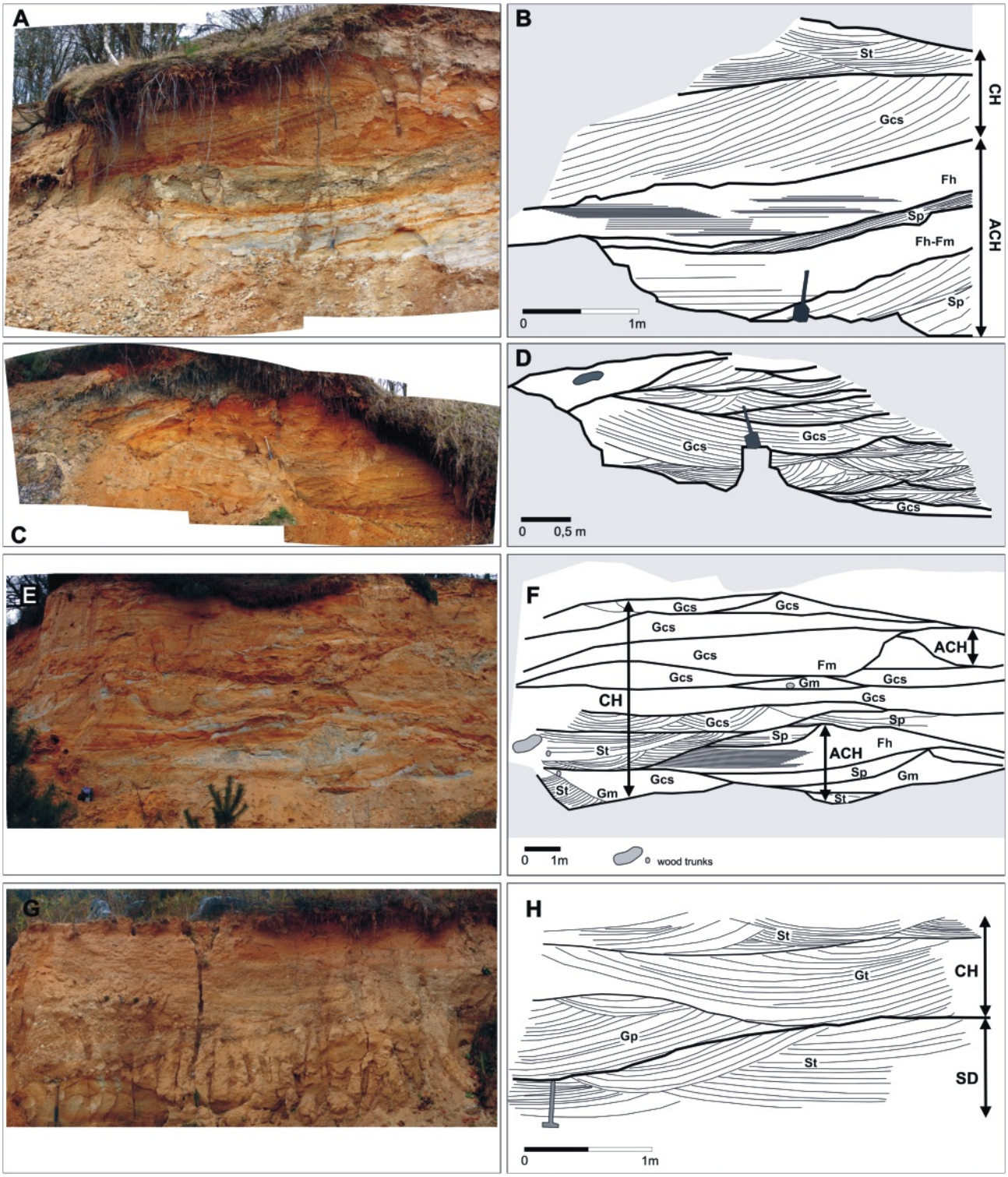

Figure 16: Photographs and line drawings documenting the facies architecture and body geometries. (A, B): infill of abandoned channel with infill of "active" channel in superposition (lower part of outcrop No. 14 - Fürwald), (C, D): complex channel infill – alternation of facies Gcs, Sp and St followed by channel abandonment (upper part of outcrop No. 14 - Fürwald), (E, F): internal structure of a channel composed of trough-shaped cross-bed sets. Smaller abandoned channel incorporated into the complex channel evolution. Notice the wood trunks in the left (outcrop No. 12 - St. Marein), (G, H): sandy dune followed by deposits of an "active" channel documenting the deposition within a broad and shallow channel (outcrop No. 9 - Thaures-E). For position of the outcrops refer to Fig. 2.

500 measurements of orientation of bounding surfaces, channel axes, foresets of cross-stratification and preferred orientation (imbrication) of pebbles. The rose diagrams were constructed according to Nemec (1988) using the EZ-Rose computer program of Baas (2000).

A complex situation of the paleotransport can be recognised within the studied area but also in individual outcrops. Differences between orientation of pebble imbrication, foresets of the cross-stratification, bar accretion and channel axis are known also in literature (Ramos and Sopeńa, 1983; Hein, 1984) and are very typical for highly mobile, rapidly shifting mid-channel bedforms and channels with highly varying water discharge.

The orientations of the channel axes are generally towards the north and northeast in the western part of the area under study. It shifts towards the east in the central parts and turns toward SSE and SSW in the eastern and southern part of the area under study.

The orientation of the accretion surfaces is mainly oblique to perpendicular to the channel axes, but also parallel orientation was recognised. Varied orientation and the existence of several bounding surfaces within one channel are the result of curved channel morphology, differences in fluvial discharge and the varied position of the dunes/bars within the channel (Bridge, 1993).

Foresets of cross-stratification are oriented generally parallel to oblique to the channel axis. More complex is their relation to the accretion surfaces. An oblique to perpendicular orientation of foresets and bounding surfaces is very often observed; parallel orientation was less common. For downstream-accretion the accretion in a direction parallel or oblique to local flow is typical. Where the orientation of the accretionary surfaces and the cross-bedding is nearly perpendicular, lateral-accretion is supposed (Miall, 1996). A significant role of lateral accretion can be followed within the SMFF depositional system. Despite this fact we suppose a braided fluvial style and not a meandering one. Lateral accretion bedding is also widespread in low-sinuosity streams indicating lateral growth and modification of mid-channel bars (Ramos and Sopeńa, 1983; Bristow, 1987; Kostic and Aigner, 2007). A varied orientation of the accretion also can be connected with different portions of the bars, i.e. upper, middle and lower ones in a braided river (Bristow, 1993).

The preferred orientation of elongated pebbles is typically perpendicular or parallel to foresets or channel axes. It reflects upstream imbrication in bars and along-stream orientation within the channels.

Interpretation: The combination of various paleocurrent data reflects that the general transport direction within the studied area was from west towards east and finally towards south. The main fluvial course oriented in these directions can be supposed. Towards this trunk river some tributaries were trending. Such a tributary (or tributaries) with transport direction from south towards north can be documented approximately in the middle part of the studied area (outcrop 11).

The two main drainage patterns of foreland basins are axial drainage (parallel to the orogen) and transverse drainage. Both of these can be documented within the studied deposits of the SMFF. The general orientation of the main river course was at first subparallel with the Alpine front (with perpendicular orientation of the tributaries), and finally perpendicular to the Alpine front. An axial drainage of the distal passive margin of the foreland basin often is discussed (Garcia-Castellanos, 2002). It could be connected with the initial stages of the foreland basin formation or with the role of a forebulge. A change in the orientation of the drainage from axial to perpendicular in the distal passive margin may be connected with reactivation of

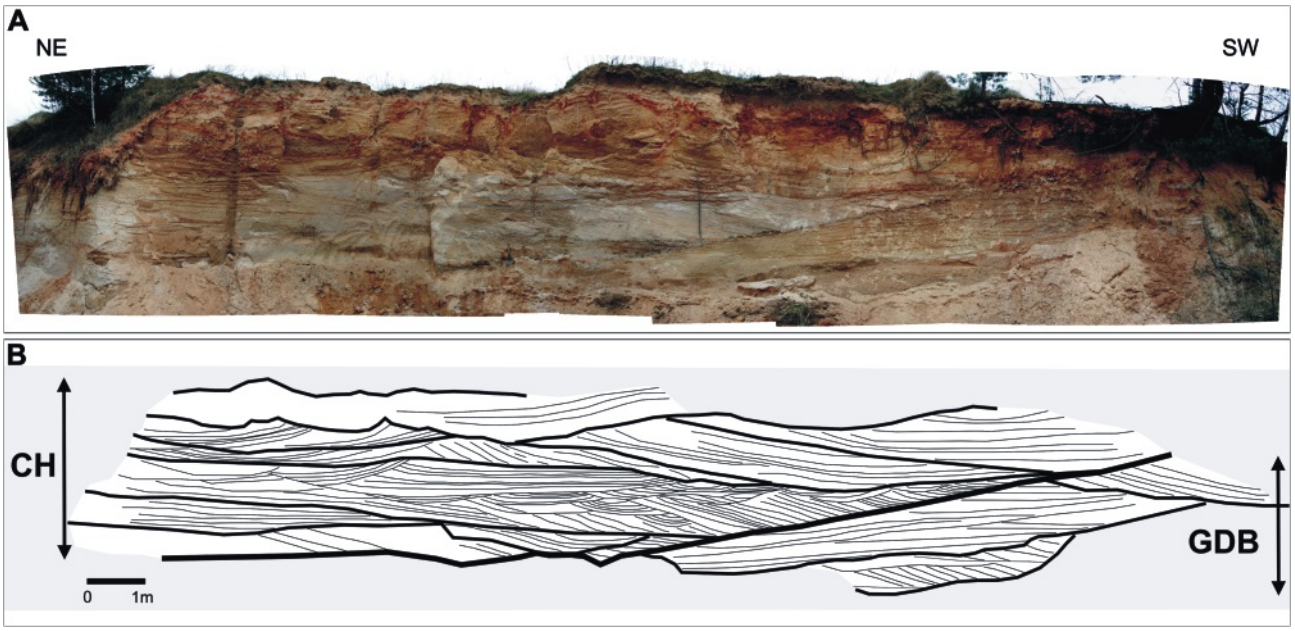

Figure 17: Photograph and line drawing documenting the facies architecture and body geometries. (A, B): deposits of gravelly channel bar laterally and vertically followed by channel infill (No. 24 - Rodingersdorf-B). For position of the outcrop refer to Fig. 2.

basement faults. The good coincidence of the position of the studied deposits and the drainage orientation along the tectonic contact of the Moldanubian zone and the Moravian zone confirms the role of basement geology and tectonics for the formation of the drainage pattern.

Moreover the drainage orientations run in directions of some of the main faults in the southeastern Bohemian Massif (i.e. N-S, W-E, WNW-ESE; cf. Roštínský and Roetzel, 2005).

7. Discussion

The facies and facies associations and the dominance of channel deposits recognised for the studied deposits of the SMFF are characteristic for a braided river environment. Steeper slopes, coarser sediments, high discharge variability and higher sediment load lead to braiding of river channels (Miall, 1978; Rust, 1984; Shukla et al., 1999). A laterally elongated lenticular geometry of the elements points to the deposition in shallow broad streams with poorly defined and easily erodible banks. Lenticular and channel-like geometry, the presence of low-angle stratified beds or mudstone filled temporarily abandoned channel facies within the channel fill succession suggest a flash-flood character of the streams or at least fluctuations in the discharge. Episodic transport, erosion and deposition are in general typical for coarse-grained rivers (Rust, 1984; Marzo et al., 1988).

The alternations of the channel fill and abandoned channel elements could reflect variations in climatic conditions, when relatively dry seasons alternated with heavy rains producing torrential floods. Typical bar and channel patterns are formed under different fluvial discharge. The morphology of elevation and depression/pools (meso-scale bedforms) is well preserved within the abandoned channels. The preserved channel deposits have a high preservation potential as they form at the lowest elevation within the channel system (Bristow et al., 1993) and hence are protected from subsequent reworking. A relatively higher rate of aggradation is indicated by the preservation of depositional elements at higher topographic levels, such as chute channels and abandoned channels. The absolute dominance of channel sediments and almost an absence of overbank deposits suggest either a low rate of sediment aggradation outside of channels or erosion due to lateral migration of channel tracts.

The results of provenance study (pebble petrography, heavy minerals), evaluation of pebble size, shape and roundness and paleocurrent data all suggest the existence of two separate parts of a fluvial system, i.e. „a main part" and a „southeastern part".

The main part system is represented by the outcrops 1- 30. A general transport from west to east, which finally (broader surroundings of Horn) turned towards the south, following today's morphology of the Horn Basin, can be supposed for this river. The west-east trending transport was connected with "transverse" tributaries both from the south and north. The principal source areas were weathered crystalline rocks of the South Bohemian Batholith and the Moldanubian zone. Local sources strongly influenced the provenance spectra. An addi-

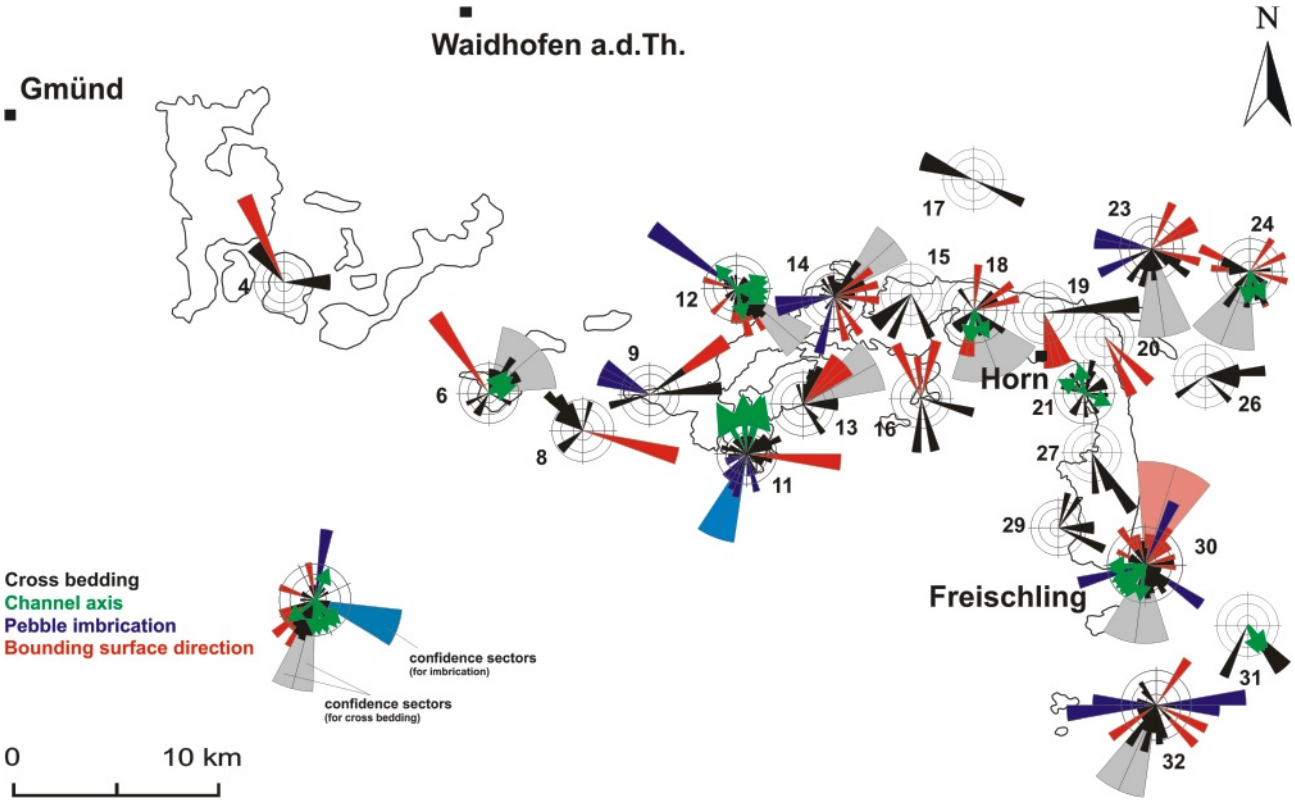

Figure 18: Orientation of bounding surfaces, channel axes, foresets of cross-stratification and preferred orientation (imbrication) of pebbles in the SMFF. Mind that No. 31 and 32 belong to the second, separate fluvial system in the southeast. For position of the outcrops refer to Fig. 2.

tional local source from reworked sediments (Mesozoic?) is supposed. The paleodrainage interpretations also point to the existence of a paleovalley trending west-east and afterwards north-south. Evidences for the confluence to the sea in an estuary are evident in the Oligocene Melk Formation south of Krems in the Statzendorf-Hermannschacht area (Roetzel et al., 1983). Due to the Lower Miocene transgression presumably the estuary was forced back to the north. Estuarine sediments with coal-bearing clays below cross-stratified sandy bars could be documented in the outcrops Maiersch (outcrop 29) and the nearby Kotzendorf north of Freischling. The position and orientation of this paleovalley is interpreted as a result of tectonic processes along the external margin of the foreland basin due to the evolution of a forebulge and a back-bulge area, as well as a consequence of a weak tectonic zone along the contact between the Moldanubian and the Moravian zones.

In the southeastern part a second fluvial system is represented by the outcrops 31 and 32. Here, a general transport direction from northeast to southwest can be documented. Metamorphic source rocks of the Moravian zone are dominating there; minor contributions come from probably Mesozoic deposits and the Thaya Batholith. This part of the fluvial system is directly located in the NE-SW trending Diendorf fault-system, where tectonic blocks with remnants of sediments of the SMFF are preserved. Due to supposed subsequent lateral strike-slip movements along this fault-system a paleogeographic reconstruction in this part is much more difficult. Therefore, the reconstruction of a possible conjunction of both recognised fluvial systems remains unclear.

The fluvial course of today´s river Kamp reveals many similarities with the studied fluvial course of the SMFF (Paleo-Kamp?). A hypothetical reconstruction of the depositional systems of the SMFF is presented in Fig. 19.

Especially in the lower parts of the fluvial system the interconnection between the fluvial course and the tectonics at the Moldanubian-Moravian boarder zone are apparent. The tectonic activity within the Eastern Alps, i.e. north-ward thrusting, probably controlled the reactivation of an ancient fault-system along the tectonic contact between the Moldanubian zone and the Moravian zone. Tectonic processes were the principal controlling factors of the formation of the paleovalleys and the slope.

8. Conclusions

The sandy and gravelly deposits of the St. Marein-Freischling Formation (Oligocene-Lower Miocene) are products of a fluvial environment reflecting the style of a braided river. A network of relatively shallow streams is characterized by fluctu-

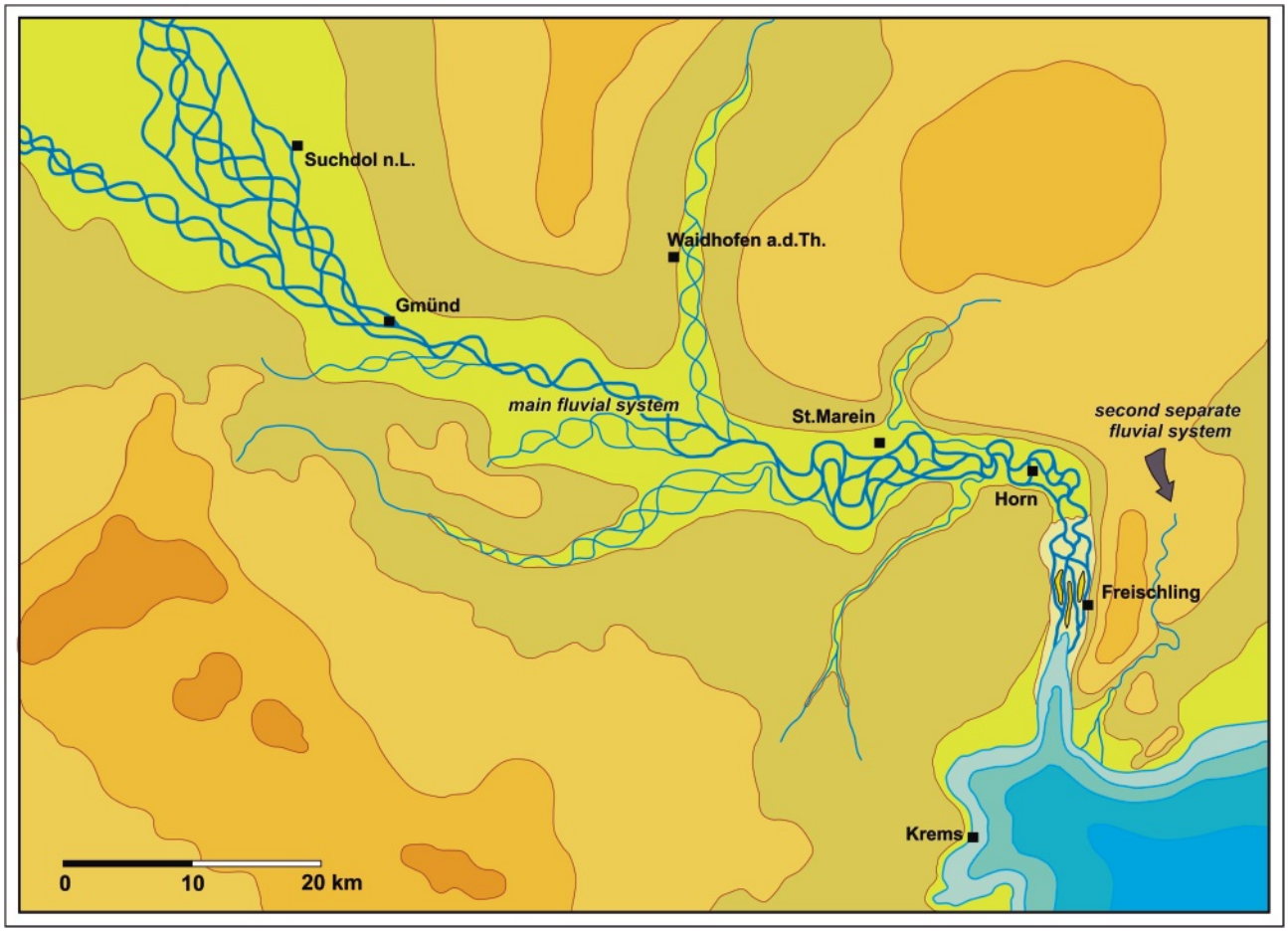

Figure 19: Hypothetical reconstruction of the fluvial system of the SMFF. In the sketch-map the paleogeographic situation in the final depositional stage in the early Early Miocene (Late Egerian) is shown.

ations in the water discharge, which controlled the episodic transport, erosion and deposition. Eleven lithofacies and four facies associations/architectural elements (gravelly channel dunes and bars, channels, sandy channel dunes and abandoned channels) were recognised.

Provenance and paleocurrent studies document the existence of two parts of the fluvial system. A general transport from west to east, which was finally (in the surroundings of Horn) diverted towards the south, can be supposed for the main part. Transverse tributaries both from north and south were connected to the west-east drained paleovalley (Fig. 19). Weathered crystalline rocks of the South Bohemian Batholith and the Moldanubian zone represented the principal source area. Local sources strongly influenced the provenance spectra. The sources precisely can be located in the Rastenberg granodiorite, Wolfshof syenitic gneiss, granulites, marbles, eclogites, amphibolites, Gföhl gneiss and possibly also Eisgarn granite. In the southeastern part of the studied area a probably separate fluvial system with a general transport direction from northeast to southwest is evident (Fig. 19), where metamorphic rocks of the Moravian zone represented the dominant provenance area, but magmatic rocks of the Thaya Batholith and probably reworked Mesozoic (?) sediments are also present.

The paleodrainage interpretation points to the existence of a paleovalley trending generally in west-east and north-south direction (Fig. 19). The position and orientation of the west-east trending part of the paleovalley is interpreted as the result of the tectonic activity (the northward thrusting of the Eastern Alps) and formation of a foreland depression along the external margin of the flexural basin (back-bulge depression?). These west-east trending paleovalley was tilted to the east, where a perpendicular north-south trending paleovalley developed along a fault separating two different units of the crystalline basement. The tectonic activity within the Eastern Alps is supposed to be responsible for the reactivation of this tectonic contact between the Moldanubian and Moravian zones.

Acknowledgements

The field works were kindly sponsored by the Geological Survey of Austria. Laboratory data were obtained with the help of the grant project of the Grant Agency of Czech Republic No. 205/09/0103. We are grateful to Hilmar v. EYNATTEN and Peter FAUPL for the constructive critical remarks in their careful reviews and to Fritz F. STEININGER for helpful discussions. David BURIÁNEK (Czech Geological Survey, Brno) contributed the geochemical data from potential crystalline source rocks and Andreas THINSCHMIDT (Krumau) provided many of the heavy mineral data.

References

Ahl, A., 2000. Klassifikation aeroelektromagnetischer Messdaten unter Verwendung von künstlichen neuralen Netzen. PhD Thesis University of Vienna, Wien, 106 pp.

Ahl, A., 2003. Automatic 1D inversion of multifrequency airborne electromagnetic data with artificial neural networks: discussion and a case study. Geophysical Prospecting, 51/2, 89-98.

Allen, P.A., Homewood, P. and Williams, G.D., 1986. Foreland basins: an introduction. International Association of Sedimentologists, Special Publications, 8, 3-12.

Ashmore, P.E., 1993. Anabranch confluence and sedimentation processes in gravel-braided streams. In: J.L. Best and C. S. Bristow (eds.), Braided Rivers. Geological Society of London, Special Publications, 75, 129-146.

Baas, J.H., 2000. EZ-ROSE: a computer program for equal-area circular histograms and statistical analysis of two-dimensional vectorial data. Computers & Geosciences, 26, 153-166.

Beaumont, C., 1981. Foreland basins. Geophysical Journal of the Royal Astronomical Society, 55, 291-329.

Best, J.L., 1988. Sediment transport and bed morphology at river confluences. Sedimentology, 35, 481-498.

Bluck, B.J., 1976. Sedimentation in some Scottish rivers of low sinuosity. Transactions of the Royal Society of Edinburgh, 70, 181-221.

Bridge, J.S., 1993. Description and interpretation of fluvial deposits: a critical perspective. Sedimentology, 40, 801-810.

Brierley, G.J., 1989. River planform facies models: the sedimentology of braided, wandering and meandering reaches of the Squamish River, British Columbia. Sedimentary Geology, 61, 17-35.

Bristow, C.S., 1987. Brahmaputra River: Channel migration and deposition. In: F.C. Ethridge, R.M. Flores and M.D. Harvey (eds.), Recent developments in fluvial sedimentology. Society of Economic Paleontologists and Mineralogists, Special Publications, 39, 63-74.

Bristow, C.S., 1993. Sedimentary structures exposed in bar tops in the Brahmaputra River, Bangladesh. In: J.L. Best and C.S. Bristow (eds.), Braided Rivers. Geological Society of London, Special Publications, 75, 277-289.

Bristow, C.S., Best, J.L. and Roy, A.G., 1993. Morphology and facies models of channel confluences. In: M. Maruo and C. Puigdefabregas (eds.), Alluvial Sedimentation. International Association of Sedimentologists, Special Publications, 17, 91-100.

Chábera, S. and Huber, K.H., 2000. Ein Beitrag zur Frage der Oberen Moldau im Tertiär. Jahrbuch des Oberösterreichischen Musealvereines, 145/1, 339-367.

Cichocki, O., 1988. Zur Histologie tertiärer Hölzer Österreichs. PhD Thesis University of Vienna, Wien, 306 pp.

Clarke, D.B., Dorais, M., Barbain, B. and Barker, D., 2004. Occurrence and origin of Andalusite in Peraluminous Felsic Igneous Rocks. Journal of Petrology, 46/3, 441-472.

Crampton, S.L. and Allen, P.A., 1995. Recognition of forebulge unconformities associated with early stage foreland basin development: example from the north Alpine foreland basin. American Association of Petroleum Geologists, Bulletin, 79, 1495-1514.

Čžjžek, J., 1849. Geognostische Karte der Umgebungen von Krems und vom Manhardsberge. Maßstab 1:72.000, Wien.

Čžjžek, J., 1853. Erläuterungen zur geologischen Karte der Umgebungen von Krems und vom Manhartsberg. Sitzungsberichte der k.k. Akademie der Wissenschaften, mathematisch-naturwissenschaftliche Classe, Beilage, 7, 77 pp.

D'Amico, C., Rottura, A., Bargossi, G.M. and Nannetti, M.C., 1982/83. Magmatic genesis of andalusite in peraluminous granites. Examples from Eisgarn type granites in Moldanubikum. Rendiconti della Società Italiana di Mineralogia e Petrologia, 38/1, 15-25.

DeCelles, P.G. and Giles, K. A., 1996. Foreland basin systems. Basin Research, 8, 105-123.

Dickinson, W.R., 1985. Interpreting provenance relations from detrital modes of sandstone. In: G.G. Zuffa (ed.), Provenance of Arenites. D. Reidel Publication Company, 331-361.

Ellenberger, F., 1948. Métamorphisme, Silicifications et Pédogénèse en Bohême Meridionale. Annales scientifiques de l'Universite de Franche-Comte-Besancon, 3, 171 pp.

Eynatten, H., von and Gaupp, R., 1999. Provenance of Cretaceous synorogenic sandstones in the Eastern Alps: constraints from framework petrography, heavy mineral analysis, and mineral chemistry. Sedimentary Geology, 124, 81-111.

Finger, F., Frasl, G., Haunschmid, B., Matl, H. and Steyrer, H. P., 1987. Über die Zirkontrachten in den verschiedenen variszischen Granitoiden der südlichen Böhmischen Masse (Oberösterreich). Jahrbuch der Geologischen Bundesanstalt, 129, 646-647.

Finger, F. and Haunschmid, B., 1988. Die mikroskopische Untersuchungen der akzessorischen Zirkone als Methode zur Klärung der Intrusionsfolge in Granitgebieten - eine Studie im nordöstlichen oberösterreichischen Moldanubikum. Jahrbuch der Geologischen Bundesanstalt, 131/2, 255-266.

Finger, F., Friedl, G. and Haunschmid, B., 1991. Wall-rock-derived zircon xenocrysts as important indicator minerals of magma contamination in the Freistadt granodiorite pluton, Northern Austria. Geologica Carpathica, 42/2, 67-75.

Finger, F. and von Quadt, A., 1992. Wie alt ist der Weinsberger Granit? U/Pb versus Rb/Sr Geochronologie. Mitteilungen der Österreichischen Mineralogischen Gesellschaft, 137, 83-86.

Folk, R.L. and Ward, W., 1957. Brazos River bar: A study in the significance of grain size parameters. Journal of Sedimentary Petrology, 27/1, 3-26.

Force, E.R., 1980. The provenance of rutile. Journal of Sedimentary Petrology, 50/2, 485-488.

Friedl, G., von Quadt, A. and Finger, G., 1992. Erste Ergebnisse von U/Pb Altersdatierungsarbeiten am Rastenberger Granodiorit im niederösterreichischen Waldviertel. Mitteilungen der österreichischen Mineralogischen Gesellschaft, 137, 131-134.

Fuchs, G., Kupka, E. and Steininger, F., 1984. Geologische Karte der Republik Österreich 1:50.000, 20 Gföhl. Geologische Bundesanstalt, Wien.

Füchtbauer, H., 1959. Zur Nomenklatur der Sedimentgesteine. Erdöl und Kohle, 12/8, 605-613.

Garcia-Castellanos, D., 2002. Interplay between lithospheric flexure and river transport in foreland basins. Basin Research, 14, 89-104.

Gerdes, A., Wörner, G. and Finger, F., 1998. Late-orogenic magmatism in the southern Bohemian Massif – geochemical and isotopic constraints on possible sources and magma evolution. Acta Universitatis Carolinae, Geologica, 42, 41-45.

Gerdes, A., Friedl, G., Parrish, R.R. and Finger, F., 2003. High-resolution geochronology of Variscan granite emplacement - the South Bohemian Batholith. Journal of the Czech Geological Society, 48/1-2, 53-54.

Gerdes, A., Finger, F. and Parrish, R.R., 2006. Southwestward progression of a late-orogenic heat front in the Moldanubian zone of the Bohemian Massif and formation of the Austro-Bavarian anatexite belt. Geophysical Research Abstracts, 8, 10698.

Gros, J.P., 1981. Nouveaux bois du Cenozoique d'Autriche et d'Ethiopie. Thèse de 3e cycle, Université Claude Bernard-Lyon 1, n° 1068 (inédit), 143 pp.

Gros, J.P., 1983. Nouveau bois fossile de l'Eggenburgien d'Autriche: Quercoxylon furwaldense n.sp. Revue générale de Botanique, 90, 43-80.

Gros, J.P., 1984. Étude comparative de 4 échantillons de bois fossiles de l'Eggenburgien d'Autiche, rapportés au nouveau genre Metacacioxylon n.g. et aux espèces M. marglii n.sp. et M. lemoignei n.sp. Revue générale de Botanique, 91, 35-80.

Gros, J.P., 1988. Nouveau spécimen de bois fossile de l'Oligocène d'Autriche rapporté a l'espèce Metacacioxylon lemoignei GROS 1981 emend. Nouvelles Archives du Musée d'Histoire naturelle de Lyon, 26, 19-27.

Gupta, S., 1997. Tectonic control on paleovalley incision at the distal margin of the Early Tertiary Alpine Foreland basin, Southeastern France. Journal of Sedimentary Research, 67/6, 1030-1043.

Harms, J.C., Southard, J.B., Spearing, D.R. and Walker, R.G., 1975. Depositional Environments as Interpreted from Primary Sedimentary Structures and Stratification Sequences. SEPM Short Course No. 2, Lecture Notes, Society of Economic Paleontologists and Mineralogists, 1-161.

Harper, Jr., C.W., 1984. Improved method of facies sequence analysis. In: R.G. Walker (ed.), Facies Models, Vol. 1, 2nd Edition. Geoscience Canada Reprint Series, 11–13.

Hein, F.J. and Walker, R.G., 1977. Bar evolution and development of stratification in the gravelly, braided, Kicking Horse River, British Columbia. Canadian Journal of Earth Sciences, 14, 562-570.

Hein, F.J., 1984. Deep-sea and fluvial braided channel conglomerates: a comparison of two case studies. In: E.H Koster and R.J Steel (eds.), Sedimentology of gravels and conglomerates. Canadian Society of Petroleum Geologists, Memoir, 10, 33-49.

Herndler, E., 1979. Zur Geologie und Hydrogeologie des Horner Beckens. PhD Thesis, University of Vienna, Wien, 168 pp.

Hochuli, P., 1983. Biostratigraphie und Paläoökologie palynologischer Proben aus dem Tertiär Österreichs, in Zusammenhang mit der Untersuchung von kohlehöffiger Fazies in N.Ö. Unpublished report, Zürich, 16 pp.

Hofmann, E., 1933. Verkieselte Pflanzenreste aus dem Horner Becken. In: F. Lukas and F. Moldaschl (Hrsg.), Heimatbuch des Bezirkes Horn. 1.Bd., 156-163.

Holbrook, J., 2001. Origin, genetic interrelationships, and stratigraphy over the continuum of fluvial channel-form bounding surfaces: an illustration from middle Cretaceous strata, southern Colorado. Sedimentary Geology, 144/3-4, 179-222.

Hoppe, G., 1966. Zirkone aus Granuliten. Berichte der Deutschen Gesellschaft für Geologische Wissenschaften - Reihe B: Mineralogie und Lagerstättenforschung, 11/1, 47-81.

Hubert, J.F., 1962. A zircon-tourmaline-rutile maturity index and the interdepence of the composition of heavy mineral assemblages with the gross composition and texture of sandstones. Journal of Sedimentary Petrology, 32/3, 440-450.

Humer, B., 2003. Der Weitraer Pluton im nordwestlichen Waldviertel (Niederösterreich). Diplomarbeit an der naturwissenschaftlichen Fakultät Universität Salzburg, 157 p.

Ilgar, A. and Nemec, W., 2005. Early Miocene lacustrine deposits and sequence stratigraphy of the Ermenek Basin, Central Taurides, Turkey. Sedimentary Geology, 173, 233-275.

Johnson, D.D. and Beaumont, C., 1995. Preliminary results from planform kinematic model of orogen evolution, surface processes and the development of clastic foreland basin stratigraphy. In: S.L. Dorobek and G.M. Ross, (eds.), Stratigraphic evolution of foreland basins. SEPM Special Publication, 52, 1-24.

Jordan, T.E., 1981. Thrust loads and foreland basin evolution, Cretaceous, western United States. American Association of Petroleum Geologists, Bulletin, 65, 2506-2520.

Klötzli, U.S., 1993. Einzelzirkon $^{207}Pb/^{206}Pb$-Datierungen an Gesteinen der Südlichen Böhmischen Masse (Rastenberger Granodiorit, Weinsberger Granit). Mitteilungen der Österreichischen Mineralogischen Gesellschaft, 138, 123-130.

Klötzli, U.S. and Parrish, R.R., 1996. Zircon U/Pb and Pb/Pb geochronology of the Rastenberg granodiorite, South Bohemian Massif, Austria. Mineralogy and Petrology, 58, 197-214.

Klötzli, U., Frank; W., Scharbert, S. and Thöni, M., 1999. Evolution of the SE Bohemian Massif based on geochronological data – a review. Jahrbuch der Geologischen Bundesanstalt, 141/4, 377-394.

Klötzli, U.S., Koller, F., Scharbert, S. and Höck, V., 2001. Cadomian lower-crustal contributions to Variscan granite petrogenesis (South Bohemian Pluton, Austria): Constraints from zircon typology and geochronology, whole-rock, and feldspar Pb-Sr isotope systematics. Journal of Petrology, 42/9, 1621-1642.

Knobloch, E., 1977. Fossile Pflanzenreste aus der Kreide und dem Tertiär von Österreich. Verhandlungen der Geologischen Bundesanstalt, 1977/3, 415-426.

Knobloch, E., 1981. Pflanzenreste aus dem Tertiär von Horn. Verhandlungen der Geologischen Bundesanstalt, 1981/2, 59-71.

Kostic, B. and Aigner, T., 2007. Sedimentary architecture and D ground-penetrating radar analysis of gravelly meandering river deposits (Neckar Valley, SW Germany). Sedimentology, 54, 789-808.

Krumbein, W.C. and Dacey, M.F., 1969. Markov Chains and embedded Markov Chains in geology. Mathematical Geology, 1, 79-96.

Leeder, M.R., 1999. Sedimentology and Sedimentary Basins. Blackwell, Oxford, 608 pp.

Lihou, J.C. and Mange-Rajetzky, M.A., 1996. Provenance of the Sardona Flysch, eastern Swiss Alps: example of high-resolution heavy mineral analysis applied to an ultrastable assemblage. Sedimentary Geology, 105, 141-157.

Lindsey, D.A., Langer, W.H. and Knepper JR. D.H., 2005. Stratigraphy, lithology, and sedimentary features of Quaternary alluvial deposits of the South Platte River and some of its tributaries east of the Front Range, Colorado. U.S. Geological Society Professional Paper, 1705.

Lindsey, D.A., Langer, W.H. and Vangosen, B.S., 2007. Using pebble lithology and roundness to interpret gravel provenance in piedmont fluvial systems of the Rocky Mountains, USA. Sedimentary Geology, 199, 223-232.

Lunt, I.A., Bridge, J.S. and Tye, R.S., 2004. A quantitative three-dimensional depositional model of gravelly braided rivers. Sedimentology, 51, 377-414.

Mader, D., 1980. Weitergewachsene Zirkone im Bundsandstein der Westeifel. Der Aufschluss, 31, 163-170.

Marren, P.M., 2001. Sedimentology of proglacial rivers in eastern Scotland during the Late Devensian. Transactions of the Royal Society of Edinburgh. Earth Sciences, 92, 149–171.

Marzo, M., Nijman, W. and Fabregas, C., 1988. Architecture of the Castissent fluvial sheet sandstones, Eocene, South Pyrenees, Spain. Sedimentology, 35, 719-738.

McLaurin, B. and Steel, R.J., 2007. Architecture and origin of an amalgamated fluvial sheet sand, lower Castelgate Formation, Book Cliff, Utah. Sedimentary Geology, 197, 291-311.

Meinhold, G., Anders, B., Kostopoulos, D. and Reischmann, T., 2008. Rutile chemistry and thermometry as provenance indicator: An example from Chios Island, Grece. Sedimentary Geology, 203, 98-111.

Miall, A.D., 1978. Lithofacies types and vertical profile models in braided river deposits: a summary. In: A.D. Miall (ed.), Fluvial Sedimentology. Canadian Society of Petroleum Geologists, Memoir, 5, 597-604.

Miall, A.D., 1985. Architectural-element analysis: a new method of facies analysis applied to fluvial deposits. Earth Science Review, 22, 261-308.

Miall, A.D., 1989. Architectural elements and bounding surfaces in channelized clastic deposits: notes on comparisons between fluvial and turbiditic systems. In: A.Taira and F. Masuda (eds.), Sedimentary Facies in the Active Plate Margins. Terra Scientific Publishing Company, Tokyo, 3-15.

Miall, A.D., 1996. The Geology of Fluvial Deposits. Springer Verlag, Berlin, 582 pp.

Mills, H.H., 1979. Downstream rounding of pebbles – A quantitative review. Journal of Sedimentary Petrology, 49, 295-302.

Montel, J.M., Foret, S., Veschambre, M., Nicollet, C. and Provost, A., 1996. Electron microprobe dating of monazite. Chemical Geology, 131, 37-53.

Morton, A.C., 1985. Heavy minerals in provenance studies. In: G.G. Zuffa (ed.), Provenance of Arenites. D. Reidel Publication Company, 249-277.

Morton, A.C., 1991. Geochemical studies of detrital heavy minerals and their application to provenance research. In: A.C. Morton, S.P. Todd and P.D.W. Haughton (eds.), Developments in Sedimentary Provenance Studies. Geological Society Special Publications, 57, 31-45.

Morton, A.C. and Hallsworth, C., 1994. Identifying provenance-specific features of detrital heavy mineral assemblages in sandstones. Sedimentary Geology, 90, 241-256.

Müller, G., 1961. Das Sand-Silt-Ton Verhältnis in rezenten marinen Sedimenten. Neues Jahrbuch für Mineralogie, Monatshefte, 1961, 148-163.

Nemec, W., 1988. The shape of the rose. Sedimentary Geology, 59, 149-152.

Nemec, W. and Postma, G., 1993. Quaternary alluvial fans in southwestern Crete: sedimentation processes and geomorphic evolution. In: M. Marzo and C. Puigdefabregas (eds.), Alluvial Sedimentation. IAS Special Publication, 17, 235-276.

Nemec, W., 2005. Principles of lithostratigraphic logging and facies analyses. Institutt for geovitenskap, University of Bergen, 1-28.

Niedermayr, G., 1967. Die akzessorischen Gemengteile von Gföhler Gneis, Granitgneis und Granulit im niederösterreichischen Waldviertel. Annalen des Naturhistorischen Museums Wien, 70, 19-27.

Parrish, R.R., 1990. U-Pb dating of monazite and its application to geological problems. Canadian Journal of Earth Sciences, 27, 1432-1450.

Pettijohn, F.J., Potter, P.E. and Siever, R., 1987. Sand and Sandstone. Springer-Verlag, Berlin, 533 pp.

Pober, E. and Faupl, P., 1988. The chemistry of detrial chromian spinels and its implications for the geodynamic evolution of the Eastern Alps. Geologische Rundschau, 77/3, 641-670.

Poldervaart, A., 1950. Statistical studies of zircon as a criterion in granitization. Nature, 165, 574-575.

Powers, M.C., 1982. Comparison chart for estimating roundness and sphericity. AGI Data Sheet 18.

Pupin, J.P., 1980. Zircon and Granite Petrology. Contributions to Mineralogy and Petrology, 73, 207-220.

Pupin, J.P., 1985. Magmatic zoning of hercynian Granitoids in France based on Zircon Typology. Schweizerische Mineralogische und Petrographische Mitteilungen, 65, 29–56.

Ramos, A. and Sopeña, A., 1983. Gravel bars in low sinuosity streams (Permian and Triassic, central Spain). IAS Special Publication, 6, 301-312.

Reading, H.G. (ed.), 1996. Sedimentary environments: Processes, Facies and Stratigraphy. Blackwell Scientific Publications, Oxford, 593 pp.

Reid, I. and Frostick, L.E., 1987. Towards a better understanding of bedload transport. In: F.G. Etheridge, R.M. Flores and M.D. Harvey (eds.), Recent Developments in Fluvial Sedimentology. Society of Economic Paleontologists and Mineralogists, Special Publications, 39, 13-20.

Roetzel, R., Hochuli, P. and Steininger, F., 1983. Die Faziesentwicklung des Oligozäns in der Molassezone zwischen Krems und Wieselburg (Niederösterreich). Jahrbuch der Geologischen Bundesanstalt, 126/1, 129-179.

Roetzel, R. and Steininger, F.F., 1991. Haltepunkt 24: Breiteneich Südost. In: R. Roetzel (Hrsg.), Geologie am Ostrand der Böhmischen Masse in Niederösterreich. Schwerpunkt Blatt 21 Horn. Arbeitstagung der Geologischen Bundesanstalt 1991, Eggenburg, 16.-20.9.1991, 210-211.

Roetzel, R., Mandic, O. and Steininger, F.F., 1999. Lithostratigraphie und Chronostratigraphie der tertiären Sedimente im westlichen Weinviertel und angrenzenden Waldviertel. In: R. Roetzel (Hrsg.), Arbeitstagung der Geologischen Bundesanstalt 1999, Retz, 3.-7.Mai 1999, 38-54.

Roštínský, P. and Roetzel, R., 2005. Exhumed Cenozoic landforms on the SE flank of the Bohemian Massif in the Czech Republic and Austria. Zeitschrift für Geomorphologie, N.F., 49/1, 23-45.

Rust, B.R., 1984. Proximal braidplain deposits in the Middle Devonian Malbaie Formation of Eastern Gaspé, Quebec, Canada. Sedimentology, 31, 675-695.

Schaffer, F.X., 1914. Die tertiären und diluvialen Bildungen. In: F.X. Schaffer, Das Miocän von Eggenburg. Abhandlungen der Geologischen Reichsanstalt, 22/4, VIII+124 pp.

Scheidegger, A.E., Figdor, H. and Aric, K., 1980. Tektonische, gravimetrische und seismische Untersuchungen in einem Senkungsgebiet der Böhmischen Masse (Niederösterreich). Archives for Meteorology, Geophysics, and Bioclimatology - Series A, 29, 167-178.

Schnabel, W., Bryda, G., Egger, H., Fuchs, G., Krenmayr, H. G., Mandl, G.W., Matura, A., Nowotny, A., Roetzel, R., Scharbert, S. and Wessely, G., 2002. Geologische Karte von Niederösterreich 1:200.000. Geologische Bundesanstalt, Wien.

Shukla, U.K., Singh, I.B., Srivastava, P. and Singh, D.S., 1999. Paleocurrent patterns in braid-bar and point-bar deposits: examples from the Ganga River, India. Journal of Sedimentary Research, 69/5, 992-1002.

Siegenthaler, C. and Huggenberger, P., 1993. Pleistocene Rhine gravel: deposits of a braided river systems with dominant pool preservation. In: J.L. Best and C.S. Bristow (eds.), Braided Rivers. Geological Society of London, Special Publication, 75, 147-162.

Slánská, J., 1967. Sedimentologie jihočeských pánví. PhD thesis Univerzita Karlova v Praze, Praha, 69-75.

Smith, S.A., 1974. Sedimentation in a meandering gravel-bed river: the River Tywi, South Wales. Geological Journal, 24, 193-204.

Sneed, E.D. and Folk, R.L., 1958. Pebbles in the lower Colorado river, Texas: a study in particle morphogenesis. Journal of Geology, 66, 114-151.

Steel, R.J. and Thompson, D.B., 1983. Structures and textures in Triassic braided stream conglomerates (´Bunter´Pebble Beds) in the Sherwood Sandstone Group, North Staffordshire, England. Sedimentology, 30, 341-367.

Steininger, F., 1968a. Bericht 1966 über Aufnahmen im Tertiär und Quartär des Horner Beckens auf Blatt 4555 (Horn). Verhandlungen der Geologischen Bundesanstalt, 1967/3, A45-A47.

Steininger, F., 1968b. Bericht 1967 über Aufnahmen im Tertiär und Quartär auf Blatt 4555 (Horn). Verhandlungen der Geologischen Bundesanstalt, 1968/3, A60-A61.

Steininger, F., 1969. Bericht 1968 über Aufnahmen im Tertiär und Quartär auf Blatt 4555 (Horn). Verhandlungen der Geologischen Bundesanstalt, 1969/3, A69-A73.

Steininger, F., 1976. Bericht 1975 über geologische Aufnahmen im Tertiär auf Blatt 21, Horn (Waldviertel). Verhandlungen der Geologischen Bundesanstalt, 1976/1, A67-A70.

Steininger, F.F., 1977. Tertiär und Quartär des Horner Beckens und des Massivrandes. Arbeitstagung der Geologischen Bundesanstalt, 1977 Waldviertel, 19-25, 72-73, 75-76.

Steininger, F., 1979. Bericht 1977 über geologische Aufnahmen im Tertiär und Quartär auf Blatt 21, Horn (Waldviertel) mit Bemerkungen zum Artikel von W. Fuchs (1977). Verhandlungen der Geologischen Bundesanstalt, 1978/1, A47-A49.

Steininger, F.F., 1983. Tertiär der weiteren Umgebung von Eggenburg, N.Ö. In: V. Höck, G. Frasl, F. Steininger and W. Vetters, Zur Geologie des Kristallins und Tertiärs der weiteren Umgebung von Eggenburg. Exkursionsführer der Österreichischen Geologischen Gesellschaft, 1, 19-25.

Steininger, F.F. and Roetzel, R., 1991. Geologische Grundlagen, Lithostratigraphie, Biostratigraphie und chronostratigraphische Korrelation der Molassesedimente am Ostrand der Böhmischen Masse. In: R. Roetzel (Hrsg.), Geologie am Ostrand der Böhmischen Masse in Niederösterreich. Schwerpunkt Blatt 21 Horn. Arbeitstagung der Geologischen Bundesanstalt 1991, Eggenburg, 16.-20.9.1991, 102-108.

Steininger, F.F., Roetzel, R. and Draxler, I., 1991a. Haltepunkt 13: Maiersch – Tongrube Frings. In: R. Roetzel (Hrsg.), Geologie am Ostrand der Böhmischen Masse in Niederösterreich. Schwerpunkt Blatt 21 Horn. Arbeitstagung der Geologischen Bundesanstalt 1991, Eggenburg, 16.-20.9.1991, 188-190.

Steininger, F.F., Roetzel, R., Pervesler, P. and Piller, W.E., 1991b. Haltepunkt 11: Oberholz – Sandgrube Hammerschmid. In: R. Roetzel (Hrsg.), Geologie am Ostrand der Böhmischen Masse in Niederösterreich. Schwerpunkt Blatt 21 Horn. Arbeitstagung der Geologischen Bundesanstalt 1991, Eggenburg, 16.-20.9.1991, 184-186.

Stendal, H., Toteu, S.F., Frei, R., Penaye, J., Njel, U.O., Bassahak, J., Nni, J., Kankeu, B., Ngako, V. and Hell, J.v., 2006. Derivavation of detrial rutile in the Yaoundé region from the Neoprotorezoic Pan-African belt in southern Cameroon (Central Africa). Journal of African Earth Sciences, 44, 443-458.

Suess, E., 1866. Untersuchungen über den Charakter der österreichischen Tertiärablagerungen. I. Über die Gliederung der tertiären Bildungen zwischen dem Mannhart, der Donau und dem äusseren Saume des Hochgebirges. Sitzungsberichte der k. Akademie der Wissenschaften, mathematisch-naturwissenschaftliche Classe, Abteilung I, 54/6, 87-149.

Triebold, S., Eynatten, H., von, Luvizotto, G.L. and Zack, T., 2007. Reconstructing source-rock lithology from detrital rutile geochemistry in the Erzgebirge (Germany). Chemical Geology, 244, 421-436.

Tucker, M. (ed.), 1988. Techniques in Sedimentology. Blackwell Science, 394 pp.

Waldmann, L., 1951. Das außeralpine Grundgebirge Österreichs. In: F.X. Schaffer (Hrsg.), Geologie von Österreich. 2. Auflage, Deuticke, Wien, 10-104.

Walker, R.G., 1975. Generalized facies model for resedimented conglomerates of turbidite association. Geological Society of America, Bulletin, 86, 737–748.

Walker, R.G., 1984. General introduction: facies, facies sequences and facies models. In: R.G. Walker (ed.), Facies Models. 2nd ed., Geosciences Canadien Reprint Series, 1, 1-9.

Walker, R.G. and James, N.P., 1992. Facies Models. Response to sea level changes. Geological Association of Canada, 380 pp.

Whiting, P.J., Dietrich, W.E. and Leopold, L.B., 1988. Bedload sheets in heterogenous sediment. Geology, 16, 105-108.

Wimmer-Frey, I., 1999. Mineralogische und granulometrische Untersuchungen an tertiären Sedimenten in den Bezirken Horn und Hollabrunn. In: R. Roetzel (Hrsg.), Arbeitstagung der Geologischen Bundesanstalt 1999, Retz, 3.-7.Mai 1999, 60-70.

Winter, J., 1981. Exakte tephrostratigraphische Korrelation mit morphologisch differenzierten Zironpopulationen (Grenzbereich Unter-/Mitteldevon, Eifel-Ardennen). Neues Jahrbuch

für Geologie und Paläontologie, Abhandlungen, 162/1, 97-136.

Zack, T., Eynatten, H., von and Kronz, A., 2004a. Rutile geochemistry and its potential use in quantitative provenance studies. Sedimentary Geology, 171, 37-58.

Zack, T., Moraes, R. and Kronz, A., 2004b. Temperature dependence of Zr in rutile: empirical calibration of a rutile thermometer. Contributions to Mineralogy and Petrology, 148, 471-488.

Zimmerle, W., 1979. Accessory Zircon from Rhyolite, Yellowstone National Park (Wyoming, U.S.A.). Zeitschrift der deutschen Geologischen Gesellschaft, 130, 361-369.

Received: 22 March 2010
Accepted: 7 October 2010

Slavomír NEHYBA[1)*)] & Reinhard ROETZEL[2)]

[1)] Institute of Geological Sciences, Faculty of Science, Masaryk University, Kotlářská 2, CZ-611 37 Brno, Czech Republic;

[2)] Geological Survey, Neulinggasse 38, A-1030 Wien, Austria;

[*)] Corresponding author, slavek@sci.muni.cz